BIOACTIVE SCAFFOLDS WITH TOPOGRAPHICAL AND BIOCHEMICAL CUES FOR VASCULAR TISSUE ENGINEERING

TAN MING HAO
(B.Eng (Hons), NUS)

A THESIS SUBMITTED
FOR THE DEGREE OF MASTER OF BIOENGINEERING
DIVISION OF BIOENGINEERING
NATIONAL UNIVERSITY OF SINGAPORE
2010

ACKNOWLEDGEMENTS

I would like to express my gratitude to my supervisor, Dr Evelyn K.F. Yim, for her tireless guidance and support throughout my course of study. I am also indebted to Dr Catherine le Visage, as well as the members of the Cardiovascular Bio-engineering Group at INSERM, for their invaluable help and advice in my experiments. Sincerest thanks to my colleagues at the Regenerative Nanomedicine Lab, for their support and contribution to enabling my experiments to be performed smoothly and successfully. Sincere thanks to Prof Colin Sheppard and Prof Toh Siew Lok, who have given me the necessary encouragement. Last but not least, I wish to extend my thanks to the various members of the bioengineering staff, including Matthew and Jacqueline, for whom this thesis would have otherwise not been possible.

TABLE OF CONTENTS

SUMMARY

Small-diameter vascular grafts face implantation problems such as thrombosis, increased rate of infection, chronic inflammatory responses and compliance mismatch between the native tissue and the prosthetic material. It has been hypothesized that a fully-endothelialized lumen would enhance biocompatibility and improve graft patency. This could be done by introducing either topographical or biochemical cues to the graft. In this study, two types of polymers were used; the polysaccharides pullulan and dextran, and a synthetic polymer, poly(vinyl alcohol) (PVA). Both material types were previously characterized as potential graft materials by Chaouat et al., in which they demonstrated short-term graft patency, although both materials were relatively inert and did not facilitate vascular tissue regeneration. The incorporation of poly-electrolyte complexation (PEC) fibers, which are known to be able to perform sustained release of various biologics, with the polysaccharide and PVA materials respectively have improved the scaffolds' abilities to perform a sustained release of proteins. PVA-PEC fiber composites further showed that mechanical strength was enhanced compared to PVA-only scaffolds. Finally, a novel method of solvent casting with PVA was developed, allowing micro- and nanometer-sized gratings to be fabricated on the surface of PVA films. Further in-vitro endothelial cell adhesion studies performed demonstrated that the grating patterns enhance adhesion of endothelial cells to the PVA surface.

LIST OF TABLES

LIST OF FIGURES

ABBREVIATIONS

BCA	Bicinchoninic acid
BSA	Bovine serum albumin
DI	Deionised
ECM	Extracellular matrix
ELISA	Enzyme-linked immunosorbent assay
HUVEC	Human umbilical vein endothelial cell
LLPAD	Lower limb peripheral artery disease
PAD	Peripheral artery disease
PBS	Phosphate buffered saline
PDMS	Polydimethylsiloxane
PEC	Polyelectrolyte complexation
PS	Polystyrene
PTFE	Polytetrafluoroethylene
PVA	Polyvinyl alcohol
STMP	Sodium trimetaphosphate
VEGF	Vascular endothelial growth factor
SEM	Scanning electron microscopy

CHAPTER 1

Introduction

1.1 Clinical Problem - Peripheral Artery Disease

Peripheral artery disease (PAD) is a type of vascular disease, categorized with disease conditions such as carotid artery, renal artery and aortic disease. PAD occurs when the arteries in the extremities, most often in the legs, experience plaque buildup within the vessel intima. Although how this happens is still unclear, the "response-to-injury" theory has been widely accepted as a probable mechanism. Endothelial injury occurs from a range of factors; oxidized low-density lipoprotein, infectious agents, toxins such as those incurred from smoking, hyperglycemia and hyper-homocystinemia. Injury typically leads to vascular inflammation and a fibro-proliferative response. Circulating monocytes enter the damaged intima and remain there, taking up low density lipoprotein cholesterol, eventually forming foam cells characteristic of early atherosclerosis. This buildup and plaque formation leads to vascular remodeling, abnormalities of blood flow and reduced oxygen supply to target organs [1].

PAD affects 12 to 20 percent of Americans over 65 years of age, with only 25 percent of PAD patients undergoing treatment [2]. In Singapore, peripheral artery disease is a major cause of limb loss [3]. It is especially prevalent in patients with diabetes, with a study in 2004 revealing that about 20% of diabetic patients over 60 years of age possess a positive history for claudication, gangrene or non-traumatic amputation as a result of PAD [4]. Although PAD can be diagnosed through symptoms such as sensations of intermittent claudication and weak systolic pressure in the limbs, a majority of PAD patients are asymptomatic or have variable non-classic PAD symptoms [2], causing pronounced difficulty in early diagnosis and prevention of the disease. For example, in Singapore, over 50% of diagnosed PAD patients are asymptomatic, while in America only an estimated 10% of PAD patients actually had classic symptoms of intermittent claudication.

Surgical bypass of occluded arterial segments had been the mainstream choice of surgical treatment in the previous decade. Use of autologous veins derived from the patient remains as the gold standard for vascular grafts in bypass surgery. Unfortunately, autologous graft sources are scarce as autologous veins are not available or inadequate in a large number of patients due to coexisting vascular diseases or previous vessel utilisation. While synthetic grafts have been used with success in large diameter arteries, considerable difficulties have been met in developing small-diameter arterial grafts with long-term patency rates.

1.2 Hypothesis

In this study, it is hypothesized that the incorporation of poly-electrolyte complexation fibers into the scaffold will enable the scaffold to release biologics at a controlled and sustained rate.

The modification of the surface topography will improve cell attachment and hence patency of the scaffold.

1.3 Aim of this Study

The objective of this study was to improve synthetic graft properties by integrating topographical properties and biochemical cues in the grafts. Two types of scaffolds already under investigation as potential graft materials were investigated in this study; poly-(vinyl alcohol) (PVA), a synthetic polymer, and a polysaccharide-based scaffold composed of the polysaccharides pullulan and dextran. To achieve this goal, the following individual strategies were applied to each of the two types of materials:

1. Integration of polyelectrolyte-complexation (PEC) fibers with the polysaccharide and PVA scaffolds was done. As PEC fibers have been shown to perform the controlled release of various biologics encapsulated in the fibers, incorporation of fibers into the scaffold would

improve the ability of the resultant composite scaffold to perform the sustained release of biologics.

2. The development of a novel method for patterning the surface of a cross-linked PVA film, to introduce surface topographical cues for endothelial cell attachment. Gratings of different dimensions were used to further determine if variations in surface topography would affect cell adhesion to the PVA film.

A summary of the experiments performed can be found in the flow chart below.

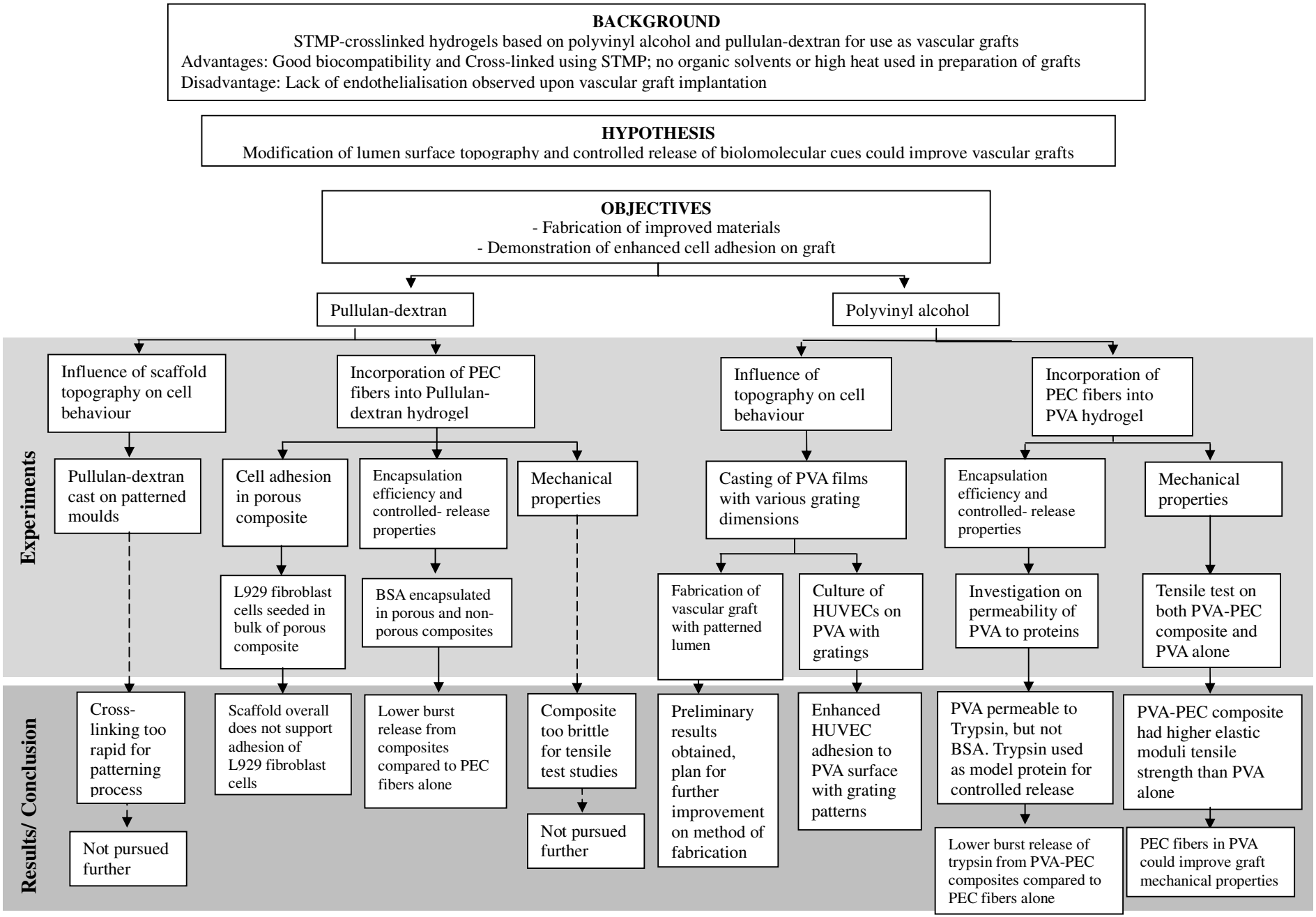
BACKGROUND
STMP-crosslinked hydrogels based on polyvinyl alcohol and pullulan-dextran for use as vascular grafts
Advantages: Good biocompatibility and Cross-linked using STMP; no organic solvents or high heat used in preparation of grafts
Disadvantage: Lack of endothelialisation observed upon vascular graft implantation
HYPOTHESIS
Modification of lumen surface topography and controlled release of biolomolecular cues could improve vascular grafts
OBJECTIVES
- Fabrication of improved materials
- Demonstration of enhanced cell adhesion on graft
Pullulan-dextran
Polyvinyl alcohol
Experiments
Influence of scaffold topography on cell behaviour
Incorporation of PEC fibers into Pullulan-dextran hydrogel
Influence of topography on cell behaviour
Incorporation of PEC fibers into PVA hydrogel
Pullulan-dextran cast on patterned moulds
Cell adhesion in porous composite
Encapsulation efficiency and controlled- release properties
Mechanical properties
Casting of PVA films with various grating dimensions
Encapsulation efficiency and controlled- release properties
Mechanical properties
L929 fibroblast cells seeded in bulk of porous composite
BSA encapsulated in porous and non-porous composites
Fabrication of vascular graft with patterned lumen
Culture of HUVECs on PVA with gratings
Investigation on permeability of PVA to proteins
Tensile test on both PVA-PEC composite and PVA alone
Results/ Conclusion
Cross-linking too rapid for patterning process
Scaffold overall does not support adhesion of L929 fibroblast cells
Lower burst release from composites compared to PEC fibers alone
Composite too brittle for tensile test studies
Preliminary results obtained, plan for further improvement on method of fabrication
Enhanced HUVEC adhesion to PVA surface with grating patterns
PVA permeable to Trypsin, but not BSA. Trypsin used as model protein for controlled release
PVA-PEC composite had higher elastic moduli tensile strength than PVA alone
Not pursued further
Not pursued further
Lower burst release of trypsin from PVA-PEC composites compared to PEC fibers alone
PEC fibers in PVA could improve graft mechanical properties

CHAPTER 2
Background - Treatment of Peripheral Artery Disease

2.1 Current treatment methods

Treatments for PAD can be divided into two categories, non-surgical and surgical. Non-surgical procedures are preferred as a fair portion of PAD patients are considered high-risk candidates for surgery. One option is a pharmaceutical approach, where patients are subjected to intravenous infusion of agents, such as anti-platelet, anti-coagulant, thrombolytic and vasoactive agents, to prevent and reduce further blockage and relieve pain [5]. Physiologically, in patients with lower limb peripheral artery disease (LLPAD), obstruction generally occurs via activation of the coagulation cascade and platelets, and they express elevated levels of fibrinogen and increased by-products of platelet degranulation. Hence, anti-coagulant and anti-platelet drugs work to augment the coagulation pathway and slow disease progression. Vasoactive agents influence the vasomotor tone of vessels. Vasodilators are thus applied in arterial disease for widening vessel diameter, improving blood flow through the affected vessel as well as reducing blood pressure.

2.2 Non-surgical approach

Of the non-pharmalogical and non-surgical approaches, physical exercise has been shown to alleviate claudication symptoms, possibly by favourably affecting the intermediary metabolism of skeletal muscle and improving oxygen extraction in the legs [6,7]. Overall, such approaches are considered conservative treatments, used to improve local blood circulation to render the limb tissue viable until natural physiological processes kick in, ideally development of collateral circulation bypassing the site of blockage. However, non-surgical treatments are ultimately done to delay surgical intervention to the limb or to supplement as post-surgical treatments, and are largely ineffective as a complete cure on their own [9].

2.3 Surgical approach

2.3.1 Amputations

In the case of surgical techniques, amputations are typically a last resort for preserving the health of a patient with critical limb ischemia, and are and are performed in the case of severe arterial disease. However, the procedure is associated with high patient morbidity, mortality and cost, and burdens the patient with a mutilative disability.

2.3.2 Endovascular surgery

As most patients are often elderly and frail with multiple coexisting health issues, minimally invasive procedures such as angioplasty and atherectomy are a preferred treatment option as opposed to undergoing open surgical revascularization, where health risks are high and recovery durations are long [11].

Balloon angioplasty and stenting are typically performed in tandem. During dilation, the surrounding plaque is fractured and the tissue media stretched with the effect of re-opening the vessel. However, the process has undesirable accompanying effects such as damage to the media, desquamation of the endothelium from stretching, as well as neointimal formation due to over-proliferation of smooth muscle cells and potential embolization [12]. In addition, plaque fractures may extend beyond the site of angioplasty treatment. All these tend to increase the risk of the entire vessel segment to restenosis or occlusion, thereby replacing one vascular problem with another.

With recent advances to improve on the long-term patency of angioplasty and stenting, drug-coated stents were introduced targeting the inhibition of neointimal formation and inflammation [13]. Two such drugs used are sirolimus and paclitaxel [14]. While both drugs have been shown to inhibit smooth muscle cell proliferation, endothelial cell proliferation is invariably inhibited as

well, leaving the stent surface exposed for thrombosis formation. In addition, metal as a stent material remains subject to inflammation and thrombosis, prompting research into biocompatible and biodegradable polymers as stent material candidates [13]. Ultimately, the goal of inhibiting neointimal hyperplasia has been acknowledged as a superficial solution to the deeper issue of encouraging positive vessel healing mechanisms.

Atherectomy involves the selective removal of atheromatous materials by cutting, pulverizing or shaving via a mechanical catheter-deliverable endarterectomy device [15], and is used for PAD patients suffering from heavily-calcified or intimal hyperplastic lesions and eccentric stenosis. However, atherectomy demonstrates no overall improvement on restenosis rates over angioplasty. The unavoidable vessel wall trauma induced from the procedure invariably leads to intimal hyperplasia, yielding poor intermediate and long-term patency rates.

As such, although endovascular surgeries have become favoured over open surgery bypasses in recent times, the frequency of surgical revascularization procedures needing secondary intervention has also increased. A population-based study in South Carolina on the impact of endovascular techniques in the recent decade has shown that, although a pronounced shift in favour of endovascular procedures over bypass surgeries, the number of secondary procedures has increased to maintain the same limb-salvage efficacies as that of the pre-endovascular era. Moreover, the number of amputations performed has not significantly changed [11]. These are indications that, although endovascular surgeries are quick, less invasive and convenient, they are still not more effective nor are they sustainable solutions to dealing with PAD compared to bypass surgery.

2.3.3 Vascular grafts

Surgical bypass of occluded arterial segments had been the mainstream choice of surgical treatment in the previous decade [16]. An open-surgery procedure, it involves the creation of a separate conduit around the blocked vessel for blood flow using a graft. Ideally, autologous vessel grafts should be used to prevent biocompatibility problems and achieve high graft patency rates [17], thus the autologous saphenous vein and mammary artery remain the gold standard for use as vascular grafts in bypass surgery [18,19]. Unfortunately, such graft sources are scarce as autologous veins are not available or inadequate in up to 40% of PAD patients, due to the typical presence of coexisting diseases such as venous thrombosis or varicose veins [17]. Other problems such as incompatible calibre and previous use [20] also limit the utilization of autologous vessels. In addition, the procedure involves an extra step of harvesting healthy vessel, thus subjecting the patient to multiple surgical procedures and making the operation more demanding and time-consuming. Relatively frail patients might not withstand the longer anaesthetic or the longer recovery time [21].

Tissue-engineered grafts were thus proposed to counter the abovementioned problems and yet maintain the biocompatibility and patency standards of the autologous vessel. Synthetic materials still posed problems of having inherent thrombogenic properties. Hence, various research groups had initially approached the problem from a wholly biocompatibility perspective, which intuitively utilized collagen or fibrin-based scaffolds seeded with native cells to mimic native vessel constituents. However it became clear that, regardless the configuration employed, the scaffolds were mechanically inferior to native arterial tissue, being unable to achieve good tensile strengths and clinically useful burst pressures [22-24]. Moreover, the tunica media of native vessels comprises an abundant amount of elastin fibers, which help prevent dynamic tissue creep and convey elastic recoil against pulsatile blood flow. Elastogenesis, or the secretion of elastin by smooth muscle cells, was generally absent in static in-vitro culture of collagen-based vessels.

Although it was later shown that mechanical stimulus, scaffold material and growth factors promoted elastin deposition to a limited extent, the mechanisms for elastin biosynthesis remain largely unknown [25].

In addition, protein-based scaffolds are susceptible to rapid degradation by the immune system [26]. As such, stronger, degradable synthetic materials such as poly(l-lactic) acid or poly(lactic-co-glycolic acid) have been brought into consideration as scaffold materials, to be eventually degraded after vessel repair and graft integration completes. Tissue-engineered grafts grown in-vitro are also subject to problems of patient cell availability, on top of requirements for logistics, time and "in house" specialist cell-culturing facilities [17]. One such method was developed by L'Heureux et al., which involved rolling cultured cells sheets together and culturing the tubular construct to recreate the three vessel layers – tunica adventitia, media and intima – in the tissue-engineered graft. Although having excellent burst pressure, the procedure required 3 months of culturing and maturation. Moreover, lack of elastin content in the matured graft led to compliance mismatch and subsequent occlusion within 7 days after implantation into dog femoral arteries [27].

With improvements to be made in the various techniques of treating PAD, synthetic grafts still occupy a substantial treatment niche; they are readily available, easily manufactured with the desired properties and relatively cheap. Since the introduction of synthetic materials for vascular grafts in the 1950s, a variety of materials have been applied and compared as vascular graft candidates, with polytetrafluoroethylene (PTFE) and Dacron emerging the most widely-used materials today. PTFE is a relatively stiff and inert fluorocarbon polymer, prepared and used as expanded PTFE by extrusion and sintering, while Dacron is a fibrous polyester that can be woven or knitted into grafts. Both materials are bioinert and do not interact with tissue, thus are used with excellent results in lower limb bypass grafts (7-9 mm). However, PTFE and Dacron grafts have poor patency and rapidly occlude when used in small-diameter arteries (<6 mm) (37).

Unfortunately, a significant number of peripheral vascular repairs below the knee involve arteries of less than 6 mm in diameter [28], greatly limiting their use in PAD treatment.

2.4 Properties influencing synthetic vascular graft patency

Surface chemistry of the graft, especially on the blood-contacting lumen surface, is crucial in graft patency. Synthetic materials have been shown to be inherently thrombogenic. This is especially so in smaller arteries where blood flow is relatively slow; plasma proteins are able to adsorb and accumulate on the graft lumen wall without being swept away by high wall shear stress, which leads to platelet adhesion to the adsorbed proteins and subsequent activation [29]. This acute response of thrombosis is followed eventually by anastomotic hyperplasia and ultimately, graft failure [30].

Two basic surface chemistry properties – electrostatic charge and surface wettability - have been shown to influence material thromboresistance. Materials such as heparin have anti-thrombogenic properties due to their hydrophilicity and net negative charge. PTFE and collagen also possess a net negative charge. However, these materials still cause platelet activation and subsequent thrombosis. Platelet activation on PTFE surfaces occur via contact activation of the coagulation cascade, starting with the adherence and autoactivation of Factor XII to the PTFE surface [8]. Collagen interacts directly with platelet receptors, or indirectly via plasma von Williebrand factor, which initiates thrombosis [10]. As such, charge is not an encompassing factor in determining thromboresistance.

As native arteries are constantly subjected to pulsatile flow forces, the criteria for graft mechanical properties are fairly stringent. Mechanical characteristics of grafts such as compliance, Young's modulus and size have considerable potential in determining graft patency [17]. Graft compliance is a widely-acknowledged benchmark for graft patency, as compliance mismatch between the graft

and vessel wall may contribute to intimal hypertrophy, turbulent blood flow and impedance mismatch or disrupted wall shear stress [32].

While compliance is a rough, endpoint measurement on a graft combining both composition and dimension, the Young's modulus gives information on only material stiffness, from which dimensions may be calculated for designing a graft with optimal mechanical properties. In this respect, materials such as Dacron and PTFE, with Young's modulus of 14 GPa [44] and 0.5 GPa [17] respectively, face graft patency problems as they are stiffer than native arteries, which are estimated to be around 0.4 MPa [33,34].

A significant difference in graft-to-host artery diameters would lead to undesirably high shear stresses, which could lead to anastomotic suture line disruption and anastomotic aneurysm formation [35]. In-vitro and in-vivo studies by Panasche et al. with prosthetic Dacron grafts showed the graft-to-host diameter ratio had to fall within the range of 1.0 to 1.4 for Dacron, while going beyond resulted in sharp increases in shear stress values [36]. Although the range varies slightly for different materials or autologous grafts, graft patency is still optimal when the difference between graft and host diameters is minimal.

CHAPTER 3

Current Developments

3.1 Materials for vascular grafts

As mentioned previously, PTFE and Dacron have long been the choice materials for current prosthetic graft implants. Expanded PTFE was first used by Matsumoto in 1973 for arterial bypass, and to date remains unrivalled in its success rate [37], although clinical long-term patency rates have remained poor for small diameter grafts [20]. Dacron grafts similarly exhibit poor performance in small-diameter vascular grafts, due to blood and vascular tissue reactivity to the material, resulting in inflammation, neointimal proliferation and inhibition of cellular regeneration [17]. Both materials have low compliance, further diminishing their potential for vascular implants [38].

Another synthetic material that has shown promise is polypropylene, which has high tensile strength (400 MPa) that can be moduluated for desired graft mechanical and biological properties by varying the fiber diameter and weaving conditions, offering an advantage over ePTFE and Dacron for small diameter vascular grafts [17]. Grafts constructed of polypropylene, which possesses greater biocompatibility and relatively low inflammatory rate, were shown to have higher patency one year after implantation compared to grafts of ePTFE or Dacron. A confluent endothelialized luminal surface was observed for the polypropylene grafts by one month [39]. The findings with polypropylene thus show the importance of the nature of the blood-contacting surface and biomechanical properties of the graft in determining patency.

Poly-(vinyl alcohol) (PVA), being biocompatible and non-thrombogenic due to its hydrophilic nature, has been a popular synthetic material candidate for biological applications ranging from contact lenses to coatings for sutures and catheters. In the field of vascular tissue engineering, various methods of crosslinking PVA have been explored in graft fabrication. One of the earliest

methods adopted was the repeated freeze-thawing of a PVA solution to physically crosslink the PVA chains and create an insoluble gel [40]. While the process is simple and straightforward, gels produced via this method tend to possess low thermal and long-term stability [41,42]. PVA chemically cross-linked with glutaraldehyde exhibits better stability than freeze-thawed PVA, however problems arise due to the residual toxicity from glutaraldehyde and subsequent leaching of cytotoxic monomers following implantation [43]. Irradiation of PVA has the advantage of sterilization and cross-linking in one step, although mechanical properties of the scaffolds yielded are relatively poor [41].

Chaouat et al. used sodium trimetaphosphate (STMP), a non-toxic compound commonly used in the food industry, to crosslink PVA in aqueous solution [44]. The resultant vascular graft exhibited excellent suture retention strength and compliance better approximating to native arterial tissue compared to PTFE and Dacron. Grafts implanted into rat aortas showed patency rates of 83% at 1 week post-implantation, with no detectable aneurysm formation. As the cross-linking process does not involve toxic components and organic solvents, the problem of residual toxicity is nullified and potential possibilities such as the incorporation of biological compounds for controlled release in the graft are open for consideration. However, the inherent hydrophilic nature of PVA does not encourage cell attachment, hence the material makes for a poor support frame for cell growth and tissue regeneration.

Natural materials, most prominently collagen, have also been considered as graft material. Although collagen is advantageous in promoting cell attachment and recellularization, it is inherently thrombogenic [45] and, with the absence of a basement membrane typically present in native arteries, would still be subject to thrombus formation. In addition, the mechanical strength of pure collagen is insufficient to satisfy graft implant criteria. A study by Berglund demonstrated that addition of elastin to collagen tubes successfully improved graft mechanical strength and

viscoelasticity [46], the latter being a long-standing problem with implanted arterial grafts. Preliminary studies have also suggested that elastin exhibits less platelet adhesion compared to collagen [47]. However, incorporating elastin with collagen in the graft fabrication process has been difficult due to the low solubility of elastin [20]. Alternatively, elastin has been successfully electrospun, using organic solvent, with polydioxane to yield grafts with good mechanical compliance and cell attachment properties [48].

Pullulan is a hydrophilic, naturally-derived polysaccharide produced from starch fermentation by the fungus *A. pullulans* [49]. Pullulan displays biochemical similarities to the extracellular matrix (ECM), thus making it non-antigenic and non-immunogenic, and hence a promising candidate for vascular grafts. Dextran, another biocompatible polysaccharide, is synthesized from sucrose by bacteria and consists of glucose units joined mostly by α 1,6-glycosidic linkages, with side chains α 1,2-, α 1,3- or α 1,4-linked to the backbone. Recently, Chaouat et al. investigated the use of a combination of pullulan and dextran polysaccharides to fabricate small diameter vascular grafts and subsequently implanted the constructs into rat aortas [50]. The growth of a pseudo-intima on the graft lumen-blood interface was observed, indicating potential in the use of the polysaccharide graft as a scaffold for vascular tissue regeneration. 80% of the implanted grafts remained patent and dimensionally stable over 8 weeks of implantation, a lower patency rate than conventional grafts. Blood clots were evidenced on the occluded grafts, indicating the limited anti-thrombogenicity of the graft. In addition, the grafts were not mechanically strong enough to withstand aortic pressures *in-vivo*, and had to be reinforced with a nylon mesh prior to implantation.

Another study was conducted by the same group on utilizing pullulan scaffolds for smooth muscle cell culture [49]. Cells were observed to express good adherence, attachment and proliferation to

the gel surface, suggesting that the scaffold could be used to regenerate the tunica media of the artery, which would greatly contribute to improving the mechanical properties of the graft. Yet another study demonstrated that the pullulan scaffolds were also conducive for endothelial progenitor cell attachment [51]. Both studies point to the potential use of pullulan grafts to regenerate both the smooth muscle and endothelial layers, which would in turn improve the thromboresistance and mechanical properties of the pullulan graft.

3.2 Endothelialization of synthetic vascular grafts

As the small diameter synthetic graft is prone to thrombosis and foreign material inflammatory response, it was proposed that a confluent layer of endothelial cells in the lumen of the graft would improve synthetic graft patency. Endothelial cells form a monolayer connected by tight junctions, and serve to prevent platelet deposition and inhibit smooth muscle cell migration to the subintimal space [28]. Moreover, the vascular endothelium also regulates physiological processes such as shear stress mechanotransduction, oxygen diffusion, macro-molecular permeability, coagulation and interaction with immune cells [52]. The vascular endothelium is essential for compensating the viscoelastic losses of the vessel wall [53]. Thus, rather than mimicking the native vessel lumen surface, introducing a confluent endothelial lining to the graft would provide thromboresistance and physiological responsiveness to the prevailing haemodynamic conditions.

In 1978, Herring et al. first reported endothelial cell seeding in grafts subsequently implanted in canine infrarenal aortas. A significantly higher rate of patency was observed, with 76% of the endothelial cell-seeded grafts remaining clot-free, compared to 22% of non-seeded ones [54]. To date, a number of methods have been devised for improving seeding endothelial cells to grafts. Such seeding methods employed include magnetic, electrostatic, vacuum and rotational cell seeding, as well as coating biological “glues” such as fibronectin on the graft lumen surface to improve cell adhesion [55,56]. However, mechanical methods of cell seeding compromise the

morphology and viability of the cells, and their requirements for long cell seeding durations pose practical limits on performing cell-harvesting and implantation on the same day, as well as prompt surgical treatment.

Another approach is to promote endothelialisation of the graft lumen after implantation. Spontaneous endothelialisation occurs by direct migration of endothelial cells from the anastomotic edge into the graft, transmural migration of endothelial cells and cell transformation from endothelial progenitor cells. Surface modification of the synthetic graft lumen with additives such as anti-CD34 antibodies and vascular endothelial growth factors has demonstrated increased endothelialisation *in-vivo* [29]. However, spontaneous endothelialisation is still a slow and limited process.

A fairly recent field of research explores how surface topography affects cell behaviour. It is generally acknowledged that cells are able to sense the stiffness and contours of its underlying surface, and by mechanotransduction, the mechanical stimulus is converted into internal chemical signalling pathways, which in turn affects cell behavioural patterns such as attachment, morphology, migration and proliferation. In endothelial cells, it was observed that surface porosity enhances endothelialisation [29], a preliminary indicator of the influence of surface roughness on endothelial cell behaviour. Another study by Zorlutuna et al. showed that nano-grating patterns improved cell retention under shear stress [57], a promising prospect in maintaining a confluent endothelium under flow conditions *in-vivo*.

In terms of cell morphology, the observed alignment of endothelial cells to linear patterns, both on the micro- and nano-scale, has been well-characterized [58-62]. The implications of this observation are not immediate, as endothelial cells typically assume a cobblestone morphology rather than an elongated one in static conditions. Cell-cell contact has also been seen to override

the influence of the underlying topography, as cells revert to the cobblestone morphology upon becoming confluent. However, probing further on the influence of topography on endothelial cell migration, the reason for cells to assume an elongated morphology becomes more apparent. Using grating patterns of 200nm depth and 2 μm groove width, Biela et al. demonstrated that human coronary artery endothelial cells not only displayed an elongated morphology along the longitudinal grating axis, but also had a tendency to migrate in the axis direction as well [58]. Similarly, Uttayarat et al. also showed that cells migrated overwhelmingly in the direction parallel to the longitudinal axis, maintaining a steady migration speed over the 4-hour course of observation. This phenomenon was enhanced in the presence of moderate to high flow [62], which implied that topography might enhance cell migration under shear force in native physiological conditions.

Although the exact cellular pathways that link cell sensing of the underlying topography to cell migration are still unknown, the mechanotactic process of endothelial cell migration in response to fluid shear stress has been better established and characterized. Embedded glycoproteins on the apical side of the cell membrane transmit the external shear stress force to align the cell's cytoskeleton [63], causing the cell cytoskeleton to elongate in the direction of the shear stresses. This in turn activates the motogenic signalling pathways in the cell, namely the Rho GTPases [64]. Cell migration thus happens when Rac, part of the Pho GTPase family, is activated and promotes actin polymerisation and hence lamellipodia protrusion in the flow direction. Rac also inhibits RhoA activity on the lagging end of the cell, inducing contraction and thus rear detachment and migration [65]. Topography thus seems to extend from the mechanotactic process of cell migration, a natural migration mechanism that occurs alongside chemotactic and haptotactic processes [64]. Along with the abovementioned effect of topography on endothelial cell behaviour, this would thus be an indication for the potential use of linear-patterned graft lumens to provide contact guidance cues for spontaneous endothelial cell migration.

3.3 Controlled release of growth factor in synthetic vascular grafts

The vascular endothelial growth factor (VEGF) family play key roles in growth and differentiation of the vasculature. The family comprises six secreted glycoproteins; VEGF-A, VEGF-B, VEGF-C, VEGF-D and placenta growth factor, of which VEGF-A plays a key functional role in angiogenesis which other VEGF family members cannot compensate for in its absence [66]. Homozygous or heterozygous deletion of the encoding gene in mice has proven embryonically lethal, resulting in vasculogenesis and cardiovascular defects [67,68], while pathological conditions involving increased angiogenesis such as psoriasis, arthritis, macular degeneration and retinopathy have been linked to VEGF-A [69].

VEGF-A is a homodimeric glycoprotein that exhibits binding affinity to both VEGFR-1 and VEGFR-2 tyrosine kinase receptors found on endothelial cells [70]. Human VEGF-A exists in six main isoforms, generated by the alternative exon-splicing of the VEGF mRNA. An important difference between each isoform is their isoelectric point and their binding affinity to heparin [71]. Of these, $VEGF_{165}$, an isoform consisting of 165 amino acids that exhibits relatively moderate affinity to heparin, has reportedly the highest biological potency amongst other variants [72,73]. Compared to $VEGF_{121}$, which has no affinity for heparin, $VEGF_{165}$ is able to bind to neuropilin-1 via its heparin-binding domain, which presents VEGF to VEGFR-1 or VEGFR-2 in a way that enhances the signal transduction cascade [70]. In contrast, $VEGF_{189}$ and $VEGF_{206}$ have relatively higher binding affinity, and thus are mostly sequestered in the extracellular matrix. Both isoforms are only released and become available upon proteolytic cleavage, an action which unfortunately simultaneously decreases their biological potency [122].

Actions of VEGF-A include stimulating microvascular permeability, endothelial cell survival, proliferation and migration [76], thus demarcating its pluripotent role in angiogenesis. Dvoark et al. proposed that, by rendering the microvasculature permeable to macromolecules, plasma proteins

such as fibrinogen and other clotting factors can leak into the extracellular space, creating a pro-angiogenic environment for endothelial cell migration [123]. Degradation of the basement membrane follows, as VEGF induces the production of matrix-degrading metalloproteinases, metalloproteinase interstitial collagenase and serine proteases [70]. VEGF-A functions as a chemoattractant for endothelial cells, specifically via extracellular gradients of VEGF-A that are generated from the secretion of VEGF in the extracellular environment and their subsequent diffusion. Such gradients have been found to induce physiological angiogenesis in the early postnatal retina [74] as well as in the developing brain and central nervous system [75]. Gerhardt et al. showed that endothelial tip cells extend their filopodia in the direction of high VEGF concentrations, while endothelial stalk cells were induced to proliferate, resulting in angiogenesis in the direction of the VEGF gradient [74].

Numerous techniques have been used to harness the effect of VEGF in inducing spontaneous re-endothelialization of synthetic grafts, namely by incorporation of VEGF in or on the surface of the graft material [75-77]. In early studies, most grafts were first synthesized before being immersed in a solution of growth factor. However, in these cases VEGF there was not much consideration for the binding or stabilizing of VEGF to the graft material, and release profiles were characterized by high initial burst releases and short release durations. In addition, VEGF is known to possess a short half-life of 1 hr in the body, an insufficient time frame for the growth factor to exert any therapeutic effect if its release was not well-controlled. The immersion-incorporation of VEGF also limited spatial control of VEGF distribution in the graft. Subsequent studies have introduced heparin as a scaffold component [78,79], as heparin forms a stable complex with VEGF, thus prolonging its half-life *in-vivo*, as well as regulating its release.

Another method of controlled release involves the encapsulation of biologics during the complexation of two polymers. When two oppositely-charged polymer solutions are brought

together, a solid fiber may be drawn at the interface of the solutions, a product of the complexation between the two polymers. The resultant fiber is known as a polyelectrolyte complexation (PEC) fiber. Should a biological compound or drug be mixed into one of the polymer solutions of similar charge to itself, the drug or compound can be drawn up during the complexation process and be subsequently encapsulated in the resultant fiber formed. This was successfully carried out by Liao et al. and Yim et al., where they demonstrated a sustained release profile of growth factors, specifically platelet-derived growth factor and transforming growth factor-β3, from a chitosan-alginate fiber construct [80,81]. Chitosan and alginate each have two ionic groups in their repeating units. During the complexation process, the negatively charged carboxylic acid groups of manuronic and guluronic acid units in alginate would interact electrostatically with the positively charged amino groups of chitosan. The controlled release of growth factor relies on the charge interactions between the polyelectrolytes and growth factor. The stability of the polyelectrolyte complex formed depends on several factors, such as drawing speed of the PEC fiber at the solution interface of the two polymers, charge density and pH. The degree of ionization can be optimized by maintaining the pH values of each polymer's solution at a specific value; chitosan in acidic solution and alginate in alkaline solution. Using chitosan with a high degree of deacetylation, and hence a high density of positive charge, also allowed for stronger electrostatic interaction.

3.4 Functionalization of PVA and pullulan-dextran vascular grafts

While PVA and pullulan both possess good biocompatibility properties, patency rates of their corresponding vascular grafts still do not satisfy clinical demands, with the abovementioned studies highlighting the occurrence of thrombosis and occlusion in implanted grafts. As mentioned previously, potential solutions to the problems are to improve cell migration and adhesion in the graft, either by introducing biolomolecular cues to the graft, providing a form of contact guidance for cell proliferation and tissue regeneration, or integrating a topographical pattern into the lumen to encourage endothelial cell migration and attachment.

Although the abovementioned studies have demonstrated that both scaffold types are biocompatible and non-thrombogenic to some degree, studies have yet to be done on using both scaffolds as vascular graft release reservoirs for growth factors. As the method of cross-linking both types of scaffolds does not involve heat or organic solvents, both scaffolds are open to a variety of modifications and incorporation of various biologics, without affecting the biocompatibility of the scaffold or concern for denaturing or degradation of fragile biological molecules.

3.5 Study objectives

The objective of this study was thus to improve and characterize synthetic graft properties by integrating topographical properties and biochemical cues in the grafts. Two types of scaffolds that were already under investigation as potential graft materials were used in this study; poly-vinyl alcohol, a synthetic polymer, and a polysaccharide-based scaffold composed of the polysaccharides pullulan and dextran. Crosslinking of either scaffold could be done using sodium trimetaphosphate (STMP), in a process that does not require the use of organic solvents or high heat. Thus, it was expected that growth factors encapsulated in scaffolds prepared in such a process would better retain their functional integrity and could be used in the grafts as biochemical cues for endothelialisation, To achieve this goal, the following individual strategies were applied to each of the two types of materials.

Firstly, integration of polyelectrolyte-complexation (PEC) fibers with the polysaccharide and PVA scaffolds was done. As PEC fibers have been shown to perform the controlled release of various biologics encapsulated in the fibers, incorporation of fibers into the scaffold would improve the ability of the resultant composite scaffold to perform the sustained release of biologics. As a preliminary investigation of the overall release profile of biologics from the composite scaffolds,

BSA and Trypsin were used as model release proteins. Subsequently, the release of vascular endothelial growth factor (VEGF), a signal peptide shown to promote endothelialisation, was also investigated in polysaccharide scaffolds.

The relatively long crosslinking duration of PVA allowed the development of a solvent-casting method for patterning the surface of PVA film, to introduce surface topographical cues for endothelial cell attachment,. Gratings patterns were chosen as gratings have been shown to facilitate endothelial cell migration. To further determine if variations in surface topography would affect cell adhesion to the PVA film, cells were seeded on a range of grating dimensions. This also served as a preliminary observation to the dimension of grating that may be optimal to the process of endothelialisation of the tubular graft lumen.

CHAPTER 4

Experimental Design

4.1 Polyelectrolyte complexation fiber fabrication

To functionalize the scaffolds for controlled release of biologics, polyelectrolyte complexation (PEC) fibers were incorporated into the polysaccharide and PVA scaffolds to form their respective composites. In this study, chitosan and alginate were the choice polymers for PEC fiber fabrication.

Chitosan was purified, following Liao et al.'s procedure [80]. Chitosan (1% w/v in 2% v/v acetic acid) was dissolved, filtered and adjusted to neutral pH with 0.5 M NaOH. The precipitated chitosan was repeatedly centrifuged at 3500 rpm for 5 min and re-suspended in DI water three times, and thereafter lyophilized for storage. The purified chitosan was then dissolved in 0.15 M acetic acid solution at 1% w/v and subsequently adjusted to pH 6 with 0.5 M NaOH. alginic powder (Sigma Aldrich) and heparin (Sigma Aldrich) were both prepared by dissolving in DI water at 1% w/v respectively.

To prepare for fiber formation, purified chitosan was dissolved in 0.15 M acetic acid solution (1% w/v) and adjusted to pH 6, while the alginic acid powder was dissolved in DI water at 1% w/v. To produce the chitosan–alginate fiber, 20 µl of chitosan solution was first brought in contact with 20 µl of alginate solution on a polystyrene dish surface. A continuous strand of fiber was drawn vertically from the solution interface by a speed-controlled motor onto either a pair of collecting needles or the PVA graft, at an approximate speed of 1 mm/s. With respect to PEC fiber incorporation into PVA grafts, heparin was additionally used in fiber formation, and alginate and heparin solution ratios were varied to a final total concentration of 1% w/v, to assess the optimum controlled release profile of growth factor from the composite construct.

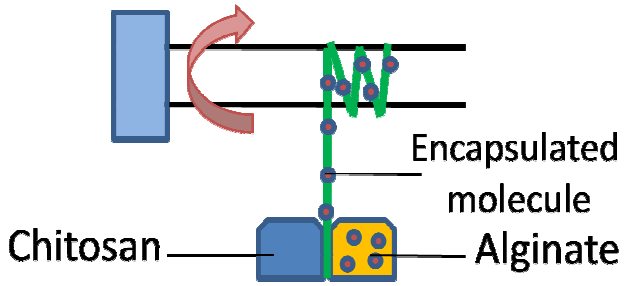

Figure 1: Set up for polyelectrolyte complexation fiber encapsulation of biologics

For encapsulation of biologics, bovine serum albumin (BSA) (Sinopharm Chemical Reagent, Shenyang, China) or VEGF (R&D Systems) were incorporated into the fibers by addition into either the chitosan or alginate solution prior to the fiber drawing. BSA, being negatively charged, was added to alginate solution at a concentration of 2.5 mg/ml, while the positively charged VEGF was added to the chitosan solution at a concentration of 2.5 µg/ml. As VEGF has shown increased binding to VEGF receptors on endothelial cells in the pH range of 7.0 to 5.5 [125], the bioactivity of VEGF could be inferred to be retained in the chitosan solution of pH 6. Addition was done in this manner to prevent premature protein-polymer aggregation before complexation. Upon completion of fiber drawing, 500 µl of phosphate buffered saline (PBS) was used to collect the remaining pool of chitosan-alginate solution, from which the concentration of remaining biologics was determined to assess encapsulation efficiency.

4.2 Polysaccharide scaffold fabrication and assessment

4.2.1 Fabrication of polysaccharide scaffold

A pre-gel mixture of pullulan/dextran 75:25 was prepared with a total concentration of 30% (w/v) in deionized (DI) water (pullulan, MW 200,000, Hayashibara Inc., Okayama, Japan; dextran MW 500,000, Sigma Aldrich). The pullulan/dextran ratio of 75:25 was adopted from an earlier study that found the ratio to be optimal to obtain mechanically compliant scaffolds for cell culture use [50]. For porous polysaccharide scaffolds, sodium bicarbonate (Sigma Aldrich) was additionally

incorporated at a concentration of 20% w/v. The mixtures were either used immediately after preparation or stored in sealed containers at 4^{o}C for later use.

One gram of the pre-gel mixture was mixed with 100 µl of 10 M sodium hydroxide (NaOH) (Sigma Aldrich) to activate the polysaccharide hydroxyl side groups for cross-linking. Chemical cross-linking of polysaccharides was carried out using sodium trimetaphosphate (STMP) (Sigma Aldrich), which was prepared in DI water at 11% w/v. Crosslinking occurs with STMP functioning as a bi-functional crosslinker between activated hydroxyl side groups of the polysaccharides. Polysaccharides mixed with STMP were then poured into a cylindrical mould of 10 mm diameter, and composite scaffolds were prepared by immersing the dried PEC fibers into the mould along with the pre-gel mix. The scaffolds were thereafter incubated at 37^{o}C for 30 minutes. Scaffolds containing sodium bicarbonate were then immersed in a 20% acetic acid solution (J.T. Baker) for 15 minutes to induce porosity. Scaffolds were thereafter washed four times with PBS to neutralize the remaining acid and remove excess reactants.

4.2.2 Controlled release studies

Controlled release studies were first performed using BSA as a model molecule, to determine whether a sustained release of biologics could be obtained from the composite scaffold of polysaccharide and PEC fibers. Once the method for encapsulation was established and optimised, VEGF was then used as the encapsulated biologic for the controlled release study. For controlled release studies using BSA, both porous and non-porous scaffolds were used in the experiment to determine any differences in release profiles between both types of scaffolds, as well as whether the extra step of inducing porosity by immersing scaffolds in acetic acid solution would affect the overall percentage encapsulation of the biologic in the scaffold.

Controlled release assessment was performed by immersing scaffolds in 1 ml of sterile PBS in a 24-well plate at 37^{o}C. A total of 250 µg of BSA was encapsulated in 100 mg of PEC fibers, while

100 ng of VEGF was encapsulated in about 40 mg of PEC fibers. In the case of VEGF controlled release studies, the release solution was prepared by dissolving 1% w/v BSA in PBS. This was done to prevent losing significant amounts of VEGF by adsorption to well surfaces and peptide degradation. At each designated assay time point, the release solution was completely drawn out and replaced with 1 ml of fresh release solution. Release solutions were stored in -80^{o}C for subsequent testing. BSA concentrations were quantified using the BCA assay kit (Pierce), and VEGF concentrations were assessed with the Duo-Set ELISA kit (R&D Systems). A total of 3 samples per scaffold type were used in the experiments.

4.2.3 Cell culture studies on polysaccharide scaffolds

Fibroblast adhesion was assessed on the polysaccharide and polysaccharide-fiber composite scaffolds, to determine if the scaffolds would be susceptible to stenosis. L929 mouse fibroblasts (ATCC, passage 20-23) were cultured with Dulbecco's modified Eagle's medium (NUMI, Singapore) supplemented with 10% fetal bovine serum (NUMI, Singapore) and 1% penicillin/ streptomycin (Sigma Aldrich). Cell cultures were washed with sterile PBS and harvested using trypsin (Gibco) from the culture flask and assessment was made of their density via haemocytometer and viability by trypan blue before cell seeding. Three different types of scaffolds; polysaccharide scaffold without fibers, scaffolds with bare fibers and scaffolds with fibronectin-incorporated fibers, were used in this study. Prior to cell seeding, scaffolds were sterilized by UV-irradiation for 1 hour. The experiment was performed in triplicates in 24-well plates. 200µl of cell suspension containing 2 x10^{5} cells was added gradually to the scaffolds and cells were allowed to adhere for 1 hour, after which each scaffold-containing well was topped up with 1 ml of fresh culture medium. The cultures were incubated at 37^{o}C with 5% CO_2 and maintained in culture for up to 1 week. Culture medium was changed daily for the duration of the experiment.

4.2.4 Scanning electron microscopy (SEM) study of scaffolds

SEM studies were carried out to assess the structure of the polysaccharide scaffolds and the morphology of the L929 cells in the scaffolds. Cacodylate buffer was prepared beforehand by preparing 0.1 M sodium cacodylate (Sigma Aldrich) and 3 mM $CaCl_2$ (Sigma Aldrich) in DI water and adjusting the solution to pH 7. After 7 days of culture, cells and scaffolds were fixed using a 2% v/v glutaraldehyde (Sigma Aldrich) solution in cacodylate buffer. Scaffolds were then washed thoroughly in cacodylate buffer solution. Ethanol dehydration was carried out by immersing scaffolds in ethanol-buffer solutions of increasing ethanol concentrations (25%, 50%, 75%, 90%, 100%). Scaffolds were then subjected to dry with hexamethyldisilazane (Sigma Aldrich), followed by sputter-coating with gold (JEOL JFC 1600 Fine Gold Coater, 10 mA, 90 secs). The surface structure and morphology of the scaffolds and cells respectively were then observed with a FEI Quanta 200F SEM.

4.3 PVA tube and film fabrication and study

4.3.1 Preparation of patterned moulds

Patterned polystyrene (PS) moulds were prepared from polydimethylsiloxane (PDMS) (Dow Corning) master templates by heat embossing. The templates prepared had patterns of parallel channels with groove and ridge widths of 10 µm and 250 nm depth, 2 µm and 2 µm depth and 250 nm with 250 nm depth. A square of PS (Corning Incorporated, Corning, NY) was heated on a hotplate to 125 ^{o}C, above the polymer's glass transition temperature. Thereafter, the PDMS master was placed pattern side facing down on the PS piece, and a constant pressure was applied for 2 minutes. The PS piece was cooled to room temperature, while maintaining the same pressure on the construct for an additional 1 minute. The patterned PS pieces were then glued with a silicone adhesive to the bottom of petri dishes (diameter 35 mm) and left to dry for 2 days before use. As a control, an additional mould was made using an unpatterned piece of PS.

4.3.2 Preparation of pre-cross-linked PVA mixture

PVA solution of 10% w/v was first prepared by dissolving 10g of PVA (Sigma-Aldrich Inc., Saint Louis, USA, 85-124 kDa; 87-89% hydrolyzed) in 100ml of distilled water and stirring at 90^{o}C until the PVA had dissolved. Temperature and stirring conditions were maintained for an additional 4 h to ensure dissolution of all aggregates and the obtained solution was then cooled to room temperature. The solution was stored at 4^{o}C until further use. STMP was dissolved in 750 µl of DI water at a concentration of 15% w/v and added to 10 ml of PVA solution, which was stirred to ensure homogeneity. 300 µl of NaOH solution at 30% w/v was then added drop-wise while stirring, and thereafter the entire solution was kept stirring constantly for 10 minutes. The pre-cross-linked mixture was used immediately after mixing.

4.3.3 Fabrication of patterned PVA films

From the pre-cross-linked mixture, 1 ml of the resultant mixture was poured into each patterned mould and centrifuged at 4000 rpm for 15 minutes to rid of bubbles in the bulk solution. The solution was thereafter degassed in a desiccator for 15 minutes, followed by another centrifugation at 4000 rpm for 1 hr to eliminate the remaining bubbles. The moulds were left at room temperature until the water was completely evaporated and a constant weight was obtained.

4.3.4 Fabrication of PVA tube scaffolds

Patterned PVA films were wet slightly with DI water and wrapped two times around a 1.7 mm diameter glass rod, patterned side facing the rod lumen. Pre-cross-linked mixture was prepared as given above, but left to stand for 2 hours until the pH fell to 8.2 prior to use. Glass rods bearing the tubes were then repeatedly dipped six times, at 10 minute intervals of drying time per dipping to allow for cross-linking, into the pre-cross-linked mixture to coat the films and form PVA tubes. For PVA tubes that were to have PEC fibers incorporated, only four dippings into the pre-cross-linked mixture were done. The newly-fabricated tubes were thereafter left on the glass rods to

cross-link overnight. Fully cross-linked tubes were washed four times in PBS at 15 minute intervals each, and the finished constructs were removed from the supporting glass rod.

4.3.5 SEM study of PVA film surface and tube lumen topography

PVA films were washed four times in PBS at 15 minutes intervals before being left to dry overnight in a fume hood. Dried films were gold sputter coated (10 mA, 90 secs) mounted, patterned side facing up, on aluminium stands for visualization by SEM. PVA tubes were also dried in a similar fashion. Prior to gold sputter coating and SEM imaging, PVA tubes were additionally freeze-fractured along their cross section at a slant angle to expose the tube lumen.

4.3.6 Permeability assessment of PVA films

As the PVA tubes were fabricated by a process that involved simultaneous evaporation and cross-linking, PVA chains within the tube scaffold would have been more densely packed compared to the polysaccharide scaffold, which undergoes a cross-linking process without evaporation. As such, it was necessary to investigate the permeability of the cross-linked PVA to macromolecules before determining the scaffold's controlled release properties. Trypsin and BSA were chosen as model molecules for this experiment as their molecular weights were of similar order of magnitude to that of VEGF (Table 1). Trypsin and BSA were also chosen due to their different charge polarities in physiological solution of pH 7.4, in order to determine if permeability of the PVA was influenced by charge polarity of the diffusing protein.

Molecule	Molecular weight (kDa)	Isoelectric point	Charge (pH 7.4)
Trypsin	23.3	10.1-10.5	Positive
BSA	66.4	4.7	Negative
VEGF	45.0	8.55	Positive

Table 1: Macromolecules of various molecular weights and charges for comparison

To assess the permeability of the PVA film to macromolecules, a diffusion chamber was set up as shown in figure 1. PVA films of 0.3±0.02 mm thickness were sandwiched between a polypropylene ring and container made from 2 ml Eppendorf tubes with the bottom cut away, leaving only the cap and locking mechanism. A 6 mm-diameter hole was cut in the cap to allow for injection of solution into the upper chamber. This created an available diffusion area for the film of about 95 mm^2. The setup was assessed for leakage by first sandwiching a piece of non-water permeable polyethylene film in the setup and filling the upper compartment with DI water. After 24 hours, the lower compartment was confirmed to have no leakage of water, thus the system was affirmed to be leak-proof.

PVA films were then used in the setup for the actual experiment. The upper compartment was filled with 300 µl of PBS solution containing 1500 ug/ml of protein. Trypsin and BSA were used as model proteins for assessing permeability, and the solutions were adjusted to pH 7.4 using 5 M sodium hydroxide solution. The lower chamber was filled with 500 µl of PBS devoid of protein. The setup was left to incubate at 37°C, and small sample volumes of 10 µl were drawn at fixed time points over 5 hours. Protein concentrations of the collected solutions were quantified using a bicinchoninic acid (BCA) assay kit (Pierce).

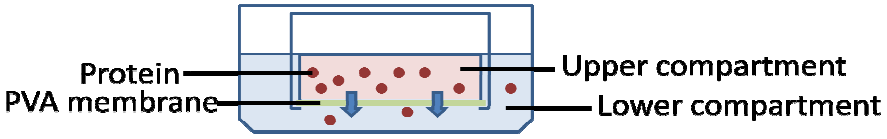

Figure 2: Set up of diffusion chamber for protein permeability assay

4.3.7 Controlled release studies for PVA tubes

Before controlled release assessment was performed for PVA-fiber composite tubes and PVA-only tubes, encapsulation efficiency of the trypsin in PEC fibers was first assessed. 180 µg of trypsin

was encapsulated in PEC fibers by mixing lyophilized trypsin (Invitrogen) in 1% w/v chitosan solution and drawing 45 µl of the solution against 45 µl of a 1% w/v solution of 90% alginate and 10% heparin. Fibers were drawn onto the thoroughly washed PVA tubes that had been subjected to only four dippings as described previously. After 2 hours of fiber-drying, PVA-fiber tubes were then subjected to an additional two dippings in cross-linked PVA solution and left to dry for another 2 hours.

The residue left behind after fiber-drawing was then dissolved and collected in 500 µl of PBS. The remaining trypsin in the residue was then quantified with the BCA protein assay kit. After encapsulation efficiency was ascertained and the amount of trypsin incorporated into the PVA-fiber construct was known, the same amount of trypsin was prepared by dissolving in 10 µl of PBS. PVA-only tubes that were previously subjected to six dippings were prepared by dehydrating thoroughly washed tubes for 2 hours in a desiccator. Thereafter, PVA tubes were each rehydrated with 10 µl of the prepared trypsin solution. Both types of scaffolds were then washed briefly with PBS for 5 minutes and immediately immersed in a 1 ml release solution of fresh PBS. At each designated assay time point, the release solution was completely drawn out and replaced with 1 ml of fresh release solution. Release solutions were stored in -80^{o}C for subsequent testing. Trypsin concentrations were quantified using the BCA assay kit (Pierce).

4.3.8 Human umbilical vein endothelial cell (HUVEC) culture and PVA film seeding

HUVEC-Cs (ATCC, 1730-CRL) were grown in EBM-2 MV growth medium (Lonza) in a humidified atmosphere at 37^{o}C, 5% CO_2, and used between passages 7-9 in experiments. Cells were washed with HEPES buffer (Lonza) and trypsinized in 0.05% trypsin (Lonza) to harvest cells. Thereafter, cell count and viability quantifications were performed with a haemocytometer and trypan blue before seeding on films. Two dimensions of films were used for this study, namely those of groove and ridge widths 2 µm and 2 µm depth, and 250 nm with 250 nm depth.

Unpatterned PVA films were used as controls in this experiment, and all samples were run in triplicate. Films were cut into 1 cm×1 cm squares, and sterilized by UV-irradiation for 20 minutes on each side before being transferred to 24-well plates. HUVECs were localized-seeded on films at a cell density of 15,000 cells/cm^2 and cultures were maintained in a humidified atmosphere at 37^oC, 5% CO_2.

4.3.9 Cell morphology studies of HUVECs on PVA films

PVA is known to resist cell adhesion. As spreading and adhesion is a pre-requisite to cells forming a congruent cell layer, this test was carried out to determine if varying the surface topography could improve cell adhesion and spread. After 24 hours of culture, cell-seeded films were washed with HEPES buffer solution and fixed for 20 minutes using a 4% paraformaldehyde solution. The washing step was then repeated and films were treated with a 1:5000 dilution of YOYO-1 (Invitrogen), a nucleic acid stain, and 10 µg/ml solution of RNAse (Invitrogen) for 2 hours in 37^oC. Subsequently, samples were washed in PBS and incubated in a 1:200 dilution of a filamentous actin indicator, phalloidin-TRITC (Invitrogen) in PBS overnight at 4^oC. Films were thereafter washed with PBS and affixed to glass coverslips using mounting medium (Fluormount, Sigma Aldrich). Stained cells were visualized using a fluorescent microscope (Leica DM IRB, Germany) and captured images were subsequently processed with the Java-based image analysis program, ImageJ (W. Rasband, http://rsb.info.nih.gov/ij/).

4.3.10 Uniaxial tensile testing

Uniaxial testing was done to determine the effects of incorporating PEC fibers on the mechanical properties of crosslinked PVA. Strips of PVA of 400 g and dimensions of 0.5 mm thickness, 3.5 mm width and 50 mm length were prepared, with the measurements taken using a pair of vernier calipers. 75 mg of PEC fibers were then spun onto each strip, aligned either perpendicular or parallel to the long axis of the strips. Thereafter, the constructs were repeatedly dipped in pre-

cross-linked PVA mixture six times at intervals of 10 minutes and left to dry overnight. The strips were then washed four times at 15 minute intervals. The dimensions of the newly-modified strips were taken and recorded again prior to testing. Uniaxial tensile testing was done on strips with parallel and perpendicular fibers, with an additional control set comprising strips with no fibers. Testing was carried out with a tabletop uniaxial testing machine (INSTRON 3345), with the use of a 10-N load cell under a cross-head speed of 10 mm/min at ambient conditions. Samples were first subjected to a pre-load of 0.1 N before measurements commenced. Four samples were tested for each type of strip-fiber configuration. Statistical significance was determined using Student's T-test.

CHAPTER 5

Results and Discussion – Fabrication and characterization of polysaccharide scaffolds

5.1 Polysaccharide scaffolds

Our focus was oriented towards characterizing the controlled release and cell growth properties of the fiber-polysaccharide construct. Polysaccharide tube-shaped scaffolds could not be made without the use of a special mould our collaborators had custom-made, which was limited in number and expensive to request for. As such, a flat, coin-shaped polysaccharide scaffold was used for experiments with the polysaccharide scaffolds.

Cross-linking of the scaffold is carried out in aqueous solution, and the general chemical reaction first involves the activation of hydroxyl groups on the polysaccharide chain and ring-opening activation of the STMP cross-linker by sodium hydroxide. Thereafter, two activated hydroxyl groups on the polysaccharide chains are covalently joined by an activated STMP molecule via two nucleophilic substitution reactions, completing the cross-linking reaction.

SEM images of polysaccharide scaffolds showed scaffolds to be highly and uniformly porous. The methodology and reagents used in preparing the scaffolds were identical to that of our collaborators [49,82,83]. In their study, polysaccharide hydrogels were characterized for scaffold porosity as a ratio of the total volume of the pores to that of the whole scaffold. Their group found pores of scaffolds prepared with this method to be lamellar and highly interconnected, with pore sizes averaging around 500 um and scaffolds overall possessing a porosity of about 50% [83].

From SEM images (Figure 3C), a close-up of the hydrogel also showed the surface to be smooth overall, and that the pore interconnectivity within the hydrogel was high. PEC fibers embedded in the polysaccharide matrix were still evident as individual strands despite being exposed to the harsh alkaline conditions, cross-linking of the surrounding hydrogel and the acidic pore-formation

process, as seen from the SEM image (Figure 3D). A higher magnification at the fiber-polysaccharide interface showed that fibers were encapsulated by the hydrogel, but both fibers and hydrogel remained separate from each other. Fiber diameters were found to average 11.0±2.2 µm, and fibers generally maintained a parallel orientation within the polysaccharide.

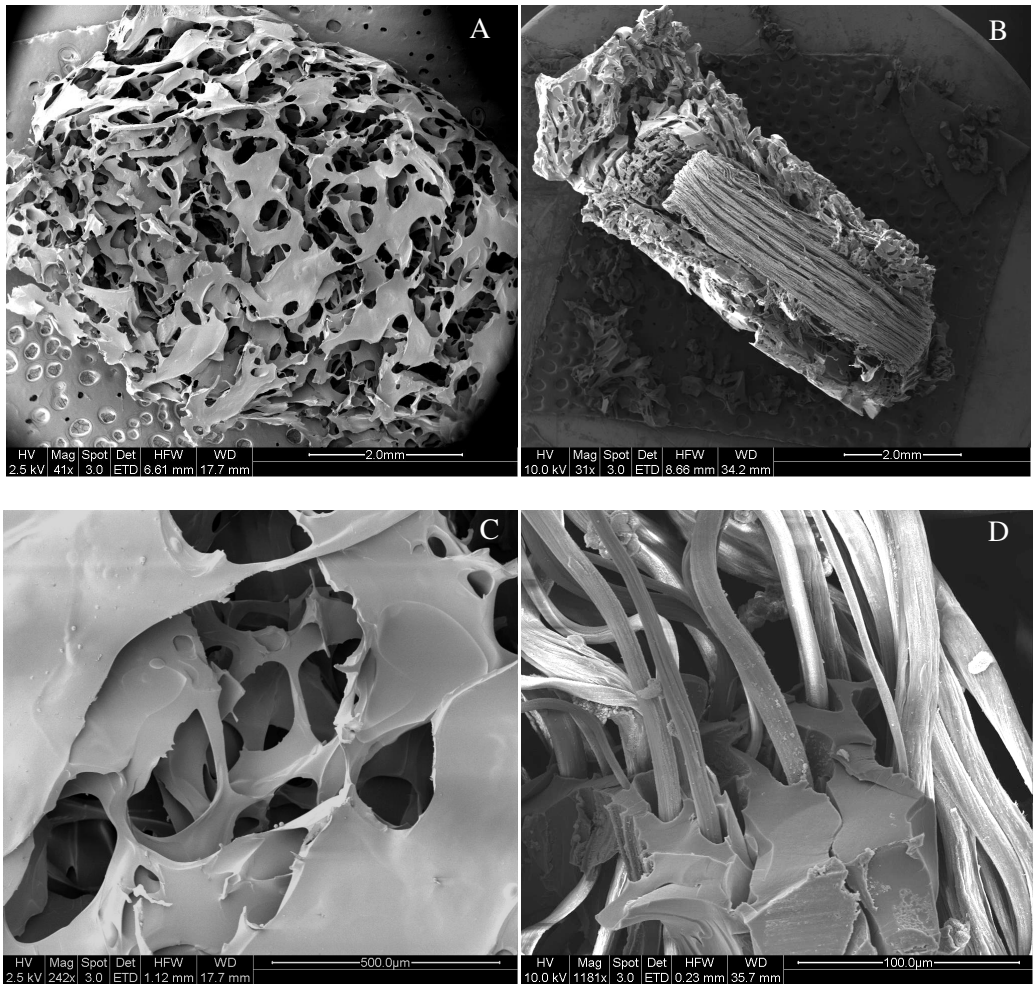

Figure 3: SEM images of porous polysaccharide scaffold (A, B) without PEC fibers and (B, D) with PEC fibers incorporated. A close-up view of (C) the gel surface and internal structure and (D) PEC fibers embedded in polysaccharide matrix

5.2 Controlled release of BSA from polysaccharide scaffolds

As SEM imaging had shown that fibers remain intact and were not significantly disrupted or diminished by the polysaccharide scaffold fabrication process, it was desired to see if the fibers could still maintain their controlled release properties as well.

While successful controlled release of biologics, including BSA, from PEC fibers was well-established by Liao et al., the release of biologics from a composite scaffold of polysaccharide gel and PEC fibers has not been investigated yet. It was thus desired to see if the composite scaffolds could serve as a controlled release platform for biologics, and how the composite scaffolds would affect the release profile compared to that of PEC fibers.

The overall encapsulation efficiency, derived from subtracting BSA remaining in the residual solution after fiber drawing from total BSA incorporated in the initial drawing solution, was around 45% ± 0.97 (data not shown). It was shown in previous work by Liao et al. that rapid drawing (10 mm/s) of the PEC fibers resulted in a higher encapsulation efficiency compared to the slower drawing process (1 mm/s), due to the formation of beads along the fiber during rapid drawing. The faster the drawing speed, the larger the beads formed. It was thus suggested that the beads acted as bulk reservoirs of the biologic encapsulates, as the complexation process was hypothesized to occur imperfectly at the beads. This further explains the higher burst release experienced by rapidly drawn fibers as the bulk reservoir of BSA in the beads are released quicker than BSA in the beadless components. Given that beadless fibers would provide a better release profile than beaded fibers, even with lower encapsulation efficiency, the fabrication of beadless fibers was still preferentially used for this study.

However, encapsulation efficiency was still lower than that reported by Liao et al., who presented a 60% encapsulation efficiency for beadless fibers. Technical problems could play a role, one notable effect being the inherent vibration of the speed-controlled motor. In their setup, the fiber-

drawing rollers were attached by means of screws to the speed-controlled motor, creating a rigid fiber-drawing setup. As the smaller needle rollers used for fiber drawing were customized to fit the polysaccharide mould thereafter, they were too small to be screwed on and were instead attached by means of sticky tape to the rotational axis of the motor and projected outwards without further support. The motor vibrations were thus amplified at the ends of the needles upon which the fiber was drawn. The vibrations caused the drawn fiber to resonate vertically, repeatedly dipping the fiber in and out of the two polymer solutions at the interface. This caused a mixing at the interface of the two solutions, causing undesirable complexation to happen within the polymer solutions. This was further evident by the visible presence of white, coagulated residue left on the plate surface after fiber drawing was completed. Polymers that had electrolytically complexed within the drawing solutions could not be incorporated into the fiber, resulting in loss of polymer and BSA on the fiber drawing surface. Attempts to suppress the motor vibrations had improved the drawing efficiency, but the vibrations could not be completely eliminated, causing the lower encapsulation rate.

Controlled release data for BSA from non-porous and porous polysaccharide scaffolds with fibers displayed a lower overall burst release compared to that of BSA released from fibers alone (Figure 4). Moreover, the porous polysaccharide scaffold displayed a relatively steadier release profile over the course of 65 days compared to the non-porous polysaccharide scaffold. This could be explained by the structural differences in both non-porous and porous polysaccharide scaffolds. It is known that solute diffusion in a scaffold is largely determined by factors such as the tortuosity, connectivity and pore size of the scaffold network. In the non-porous scaffold, mass transport of BSA is limited by the relatively small pore size of the cross-linked polysaccharide network, compared to the porous scaffold where BSA is transported through larger macropores created by gas foaming from the reaction of sodium bicarbonate with acetic acid. Furthermore, the process of gas foaming resulted in highly-interconnected channels throughout the scaffold, facilitating the

outward diffusion of BSA through such channels. As such, the release rate up to the 20-day timepoint was lower for the non-porous scaffold compared to the porous scaffold. However, a burst release from the non-porous scaffold at the 20 to 25 days interval showed that the release profile of the non-porous scaffold did not follow simple release kinetics. One possible reason was that the eventual degradation of the polysaccharide scaffold could have resulted in the burst release of BSA initially hindered by the polymer network. However, degradation studies of the scaffolds would have to be conducted to determine if this was indeed the cause of the burst release.

Overall, BSA release rates from both composite scaffolds were lower than that of the fiber scaffold, as the presence of the polysaccharide mesh would have hindered solute transport by bulk flow.

The total amount of BSA released between the three scaffolds was in the range of 41-44% over 65 days, indicating that either a negligible quantity of BSA was degraded or lost during the additional polysaccharide encapsulation process of the fiber.

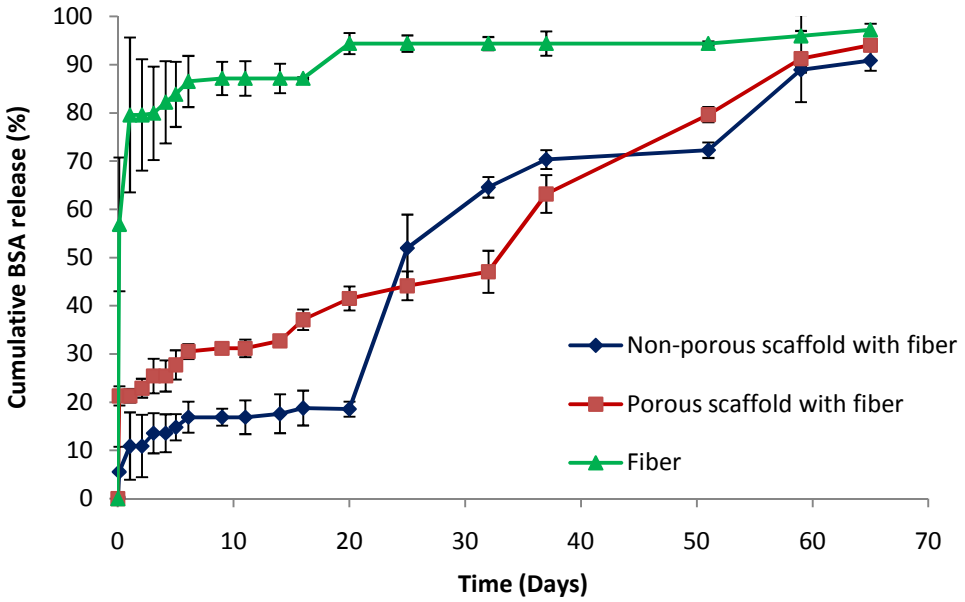

Figure 4: Graph of cumulative BSA release over 65 days from (◆) non-porous scaffolds with fibers, (■) porous scaffolds with fibers and (▲) fibers only (SD, n = 3)

Overall, it was promising to note that the BSA encapsulated was not significantly lost during the process of encapsulating the BSA-loaded fiber in polysaccharide, nor in the process of effervescence in 20% acetic acid to create the porous gel, which were the key points of investigation before moving on to perform the controlled release with VEGF.

5.3 Controlled release of VEGF from polysaccharide scaffolds

As a steady state of VEGF release is preferred for angiogenesis, the porous polysaccharide-fiber scaffold was chosen for use in the subsequent controlled release experiment using VEGF. Heparin was incorporated into the fiber, as its high density of negatively charged sulfate groups has been noted to electrostatically bind to and stabilize the positively-charged VEGF, influencing the growth factor release profile. The aim was thus to determine the optimal amount of alginate: heparin ratio for controlled release of VEGF.

The initial encapsulation efficiencies during fiber drawing of all three configurations of alginate: heparin ratios were measure by ELISA. It was noted that, with an increasing concentration of heparin, the encapsulation efficiency improved significantly.

Alginate: Heparin ratio	9:1	8:2	1:1
Encapsulation efficiency (%)	71.5±0.8	75.5±2.7	97±3.8

Table 2: Encapsulation efficiency of VEGF expressed as a percentage of the total growth factor added to the chitosan drawing solution

Notably, despite the good encapsulation efficiencies, the resultant total VEGF release quantity over 7 days was low, with an overall 5% of VEGF released by scaffolds with fibers of alginate: heparin ratios of 1:1 and 8:2 over 7 days, and only 3.2 % released by scaffolds of alginate: heparin ratios of 1:1. Furthermore, the cumulative release profile of scaffolds with fibers of an alginate: heparin ratio of 9:1 seemed to reach a plateau between 24 and 168 hours, during which negligible amounts of VEGF were released.

One possible reason was that VEGF might have strong electrostatic interactions with the sulfate groups in heparin, such that its release rate had been decreased. This was reflective of the data obtained by Liao et al. [80] for the encapsulation of PDGF-bb in 90% alginate and 10% heparin fibers. Their group had also reported a total released quantity of less than 5% from their heparin-based fibers over 25 days, compared to fibers without heparin where the release of PDGF-bb was over 50% for the same time period. Hence, it can be extrapolated that VEGF might have remained bound within the fibers, especially so for fibers, with alginate: heparin ratio of 1:1, given the high concentration of heparin incorporated.

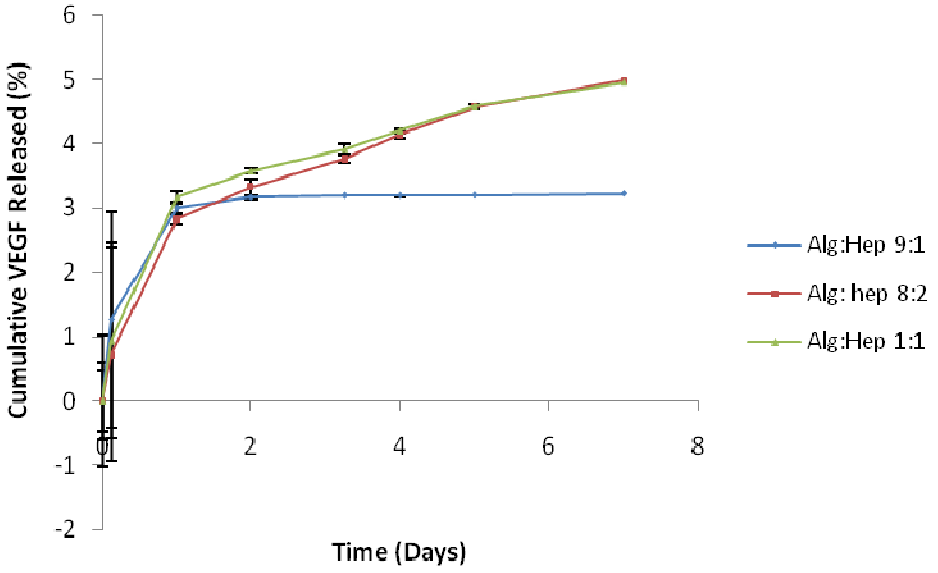

Figure 5: Graph of VEGF release from porous polysaccharide-fiber scaffold, using three different ratios of alginate: heparin, 9:1, 8:2, 1:1, for fiber formation (SD, n = 3)

In addition, the positively-charged VEGF may also have electrostatically interacted with surrounding negatively-charges of the intermolecular phosphate linkages in the polysaccharide scaffold, slowing its diffusion out of the scaffold. Typically, a phosphate functional group would possess a net negative charge of two, while the sulfate functional group, as that present on heparin, would have a smaller net negative charge of one. However, as the phosphate group in the polysaccharide scaffold functions as a cross-linker between polymer chains, two oxygen molecules of the phosphate group are involved in ester linkages, leaving a net negative charge of one per

phosphate unit in the linkage. The mechanism of cross-linking with STMP can either yield a pyrophosphate cross-link formation between polymer chains, or a monophosphate crosslink formation. In the first case two negative charges are present on the linkage, whereas in the second, one negative charge is present on the linkage. Negative charges present on both phosphate and sulfate groups in the scaffold would thus be available to interact with VEGF. The hindered diffusion of VEGF was also observed by our co-authors, who reported a significantly low overall release of VEGF from polysaccharide scaffolds similarly cross-linked with STMP and infused with a VEGF solution (publication in progress). Due to time limitations, the controlled release experiment was not continued beyond 7 days.

5.4 Cell morphology studies of L929 cultured in polysaccharide scaffolds

As a preliminary investigation, L929 mouse fibroblasts were used to assess the hydrogel-only and composite hydrogel-fiber scaffolds' cell adhesion properties. L929 fibroblasts have been a popular cell model used in assessing cell behaviour and cytotoxicity of scaffolds for tissue engineering [84-86], as they are known to be relatively easy to culture, exhibit high cell adhesiveness to substrates and possess fast proliferation rates. Successful cell adhesion is a prerequisite of proliferation for anchorage-dependent cells [127]. Hence, a scaffold that is unfavourable to L929 fibroblast growth can be generally acknowledged to have poor support for fibroblast proliferation.

As the thick hydrogel scaffold posed imaging problems with regards to autofluorescence and light scattering , it was difficult to get a clear image of individual cells using fluorescence or light microscopy. Hence, SEM was opted as the imaging technique to observe cell behaviour within the scaffold.

The seeded fibroblasts appeared dispersed throughout the volume of the scaffold. As the scaffold pore size was relatively large and the degree of interconnectivity between pores was high, cells

were able to access the bulk of the scaffold. Extended studies performed in our lab on L929 cell proliferation and viability in polysaccharide and polysaccharide-fiber composite scaffolds in a separate report [87] showed that fibroblasts in polysaccharide scaffolds remained viable and retained their proliferation capability, an indication that the polysaccharide hydrogel environment proved biocompatible and non-toxic to the cells.

In polysaccharide scaffolds with no fibers, fibroblasts tend to remain mostly spherical and grouped in clusters, an indication that the polysaccharide surface was unfavourable for L929 fibroblast attachment. Although L929 cells seeded in polysaccharide scaffolds with fibers appeared to cluster around the fibers, they remained mostly in cell clusters as well, and individual L929 fibrolasts maintained a spherical morphology. In some instances, cells were observed to exhibit guided alignment along the fiber axis (Figure 6a), although in general, cells remained spherical and did not spread well on the fiber surface.

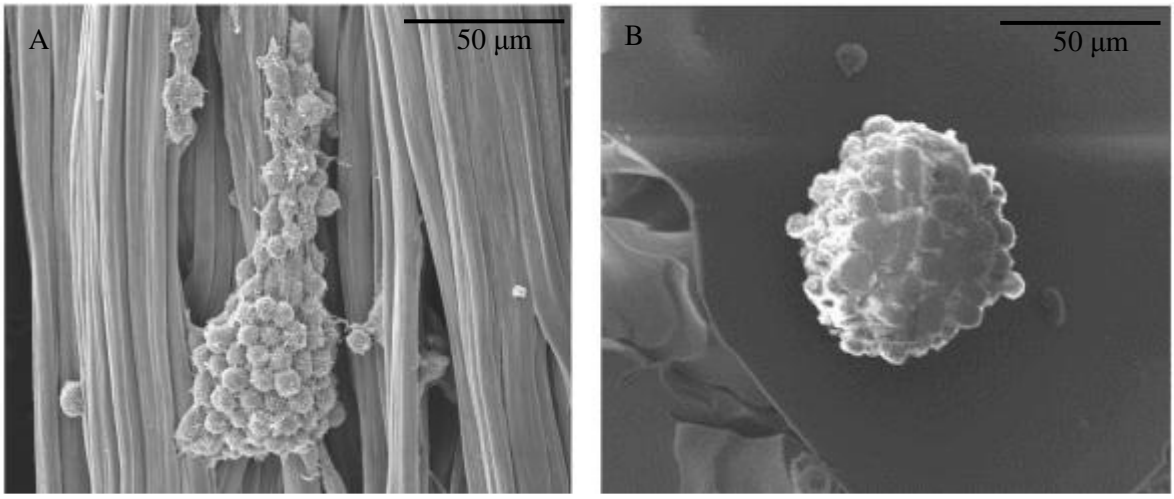

Figure 6: SEM images of fibroblasts on (A) PEC fibers of the polysaccharide-fiber composite scaffold and (B) on the hydrogel surface of the polysaccharide-only scaffold

It was previously reported that cells do not adhere well to surfaces of high hydrophilicity, preferring instead surfaces of moderate hydrophobicity [88,89], as a layer of water molecules adsorbed on the hydrophilic surface would prevent the adsorption of proteins that would otherwise

mediate cell adhesion [90]. As the polysaccharide hydrogel was reported to possess a water content of over 90% [51], the surface hydrophilicity could have been a reason for the poor cell adhesion to the hydrogel surface. In addition, the net negative charge of the polysaccharide due to the phosphate groups incorporated from STMP during cross-linking might have further discouraged cell adhesion. As cell membranes have a net negative charge, cells have been known to be attracted, and hence preferentially attach, to positively-charged surfaces [91].

With respect to fibroblast attachment to the PEC fibers, the poor attachment might have been due to the absence of extracellular matrix proteins or adhesion molecules available for interaction with the cell adhesion surface receptors. In addition, the amine groups on deacetylated chitosan, which normally facilitate cell interaction and protein deposition on the chitosan surface due to their positive charge, are involved in electrostatic interactions with the negatively-charged hydroxyl groups of alginate, further decreasing the likelihood of cell adhesion to the fiber surface.

As one of the common modes of failure of synthetic grafts is due to the formation of neo-intimal hyperplasia or stenosis, where there is undesired growth of fibroblasts or smooth muscle cells that cover the lumen of the graft [92], it is promising to see that the composite graft does not support the adherence of fibroblasts, which are amongst the cell types that express high adherence tendencies to surfaces.

CHAPTER 6

Results and Discussion - Fabrication and Characterization of PVA scaffold

6.1 SEM images of patterned PVA films

While patterning of PVA polymer by solvent-casting has been previously demonstrated [93], the patterned PVA films formed are not cross-linked and are highly unstable in water. Hence, their uses are limited to being convenient secondary moulds for pattern transfer from a master mould onto a non-water soluble substrate. The patterned PVA moulds are thus usually dissolved in water to release the non-soluble patterned substrate after its pattern replication from the PVA mould is complete.

SEM images of the patterned PVA films by SEM showed that grating patterns were successfully replicated over the entire area of the polystyrene master moulds (
Figure 8). Unlike STMP-crosslinking of the polysaccharide, the amount of sodium hydroxide used for PVA cross-linking was nearly a fifth the concentration, hence cross-linking of PVA with STMP was hypothesized to be more strongly dependent on the solvent evaporation process.

The fairly unique process of solvent-casting coupled with cross-linking employed was only possible due to the mechanism of cross-linking between PVA and STMP. The mechanism of STMP cross-linking was elaborated by Lack et al. [94] (Figure 7). Sodium hydroxide is first depleted in the reaction for PVA side chain activation and opening of the STMP ring. At the point when the reaction solution pH falls below 13, there is an accumulation of $STPP_g$ from the reaction between STMP and PVA, whereby the reaction does not proceed further. Due to both reactants $STPP_g$ and the activated hydroxyl side chain of PVA being negatively charged, it becomes quite difficult for nucleophilic substitution to take place, thus halting the initiation of cross-linking between PVA chains. However, upon evaporation, the concentration of the reagents and the alkalinity of the solution increases, allowing the reaction to continue. The negative charge and

repulsion on the α-phosphate is weaker compared to the other two phosphates in $STPP_g$, making it more susceptible to nucleophilic attacks and allowing two PVA chains to be chemically cross-linked by a phosphate bridge. As such, evaporation precedes the cross-linking reaction without interference, allowing the conventional solvent-casting process for mould replication to take place.

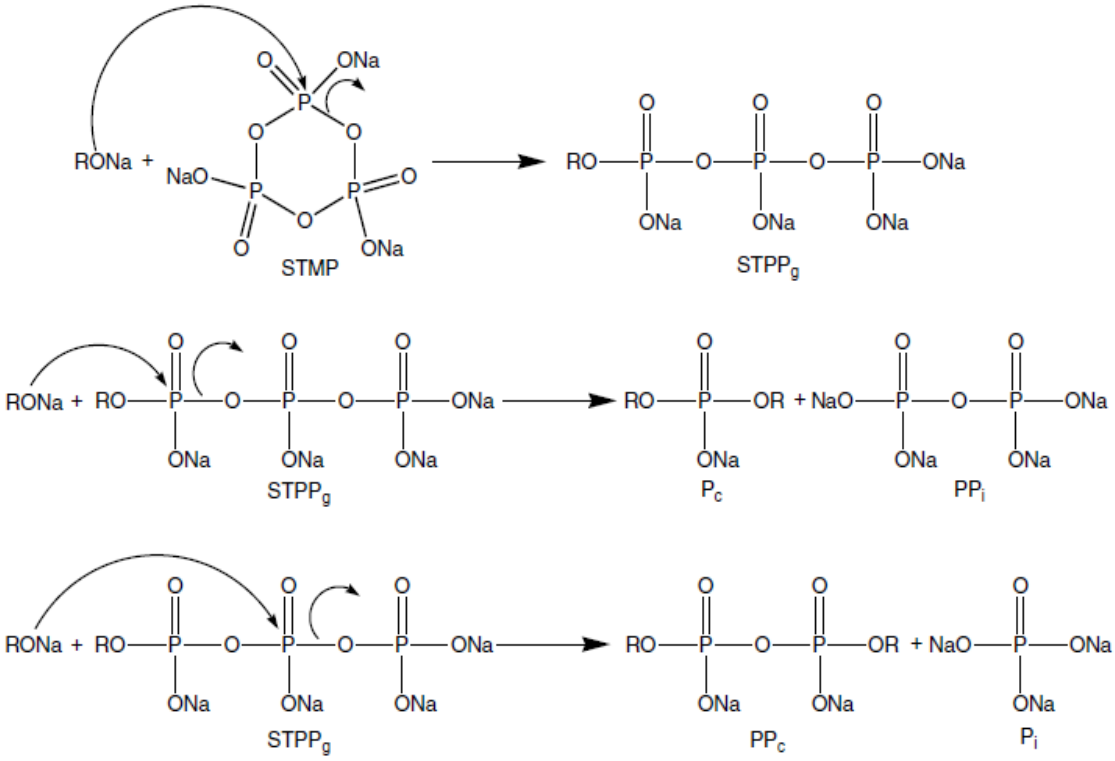

Figure 7: The reaction mechanism of the cross-linking between PVA chains with STMP, as described by Lack et al. [94]

It was noted previously that when the height of the PVA pre-cross-linked solutions in the mould were too high or when the solutions were left to evaporate too rapidly during the solvent-casting and cross-linking process, a persistent problem of hazing and blistering of the cast film surface was evident, covering most of the periphery of the pattern area. The area was typically characterized by a rough, bumpy surface with little or none of the intended pattern replicated. This was found to be a phenomenon of uneven drying throughout the thickness of the film coupled with the formation of vapour bubbles nucleating within the cast solvent [95,96]. A concentration

gradient of the polymer is created from the rapid surface evaporation, with the highest polymer concentration at the air-solution interface. The formation of a tight layer of polymer skin on the surface along with the increasing viscous thickening nearing the surface causes vapour bubbles formed in the bulk solution over time to meet with resistance when transporting out of the solvent by buoyancy or convective transport. Subsequently, the reduction of the pre-cross-linked solution depth in the mould as well as a retardation of evaporation processes was found to greatly improve the replication quality of the films, presumably by improving the uniformity of the evaporation process throughout the thickness of the solution during the solvent casting process.

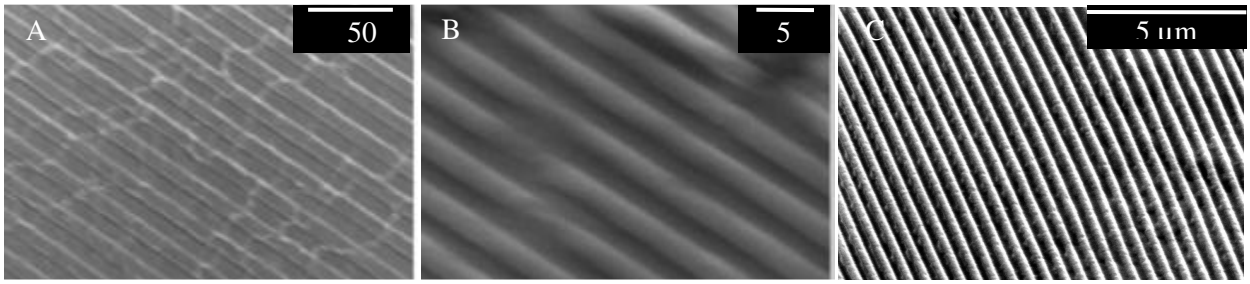

Figure 8: SEM images of patterned PVA films made from PS moulds of dimension aspects (A) 10 µm, (B) 2 µm and (C) 250 nm

The films with grating patterns of 10 µm and 2 µm aspect ratio were additionally rehydrated and immersed in PBS, where the lateral swelling of the grating ridge and groove widths in solution was measured to be about 1.2 times as much as the dehydrated films. In addition, films were tested for stability by immersion in PBS for 7 days, after which they were observed under a bright-field microscope in solution. The grating dimensions remained unchanged, and patterns maintained their structural integrity (

Figure 9). This was a promising sign that cross-linked PVA films were able to sufficiently maintain their surface topography in physiological solution for prolonged periods of time.

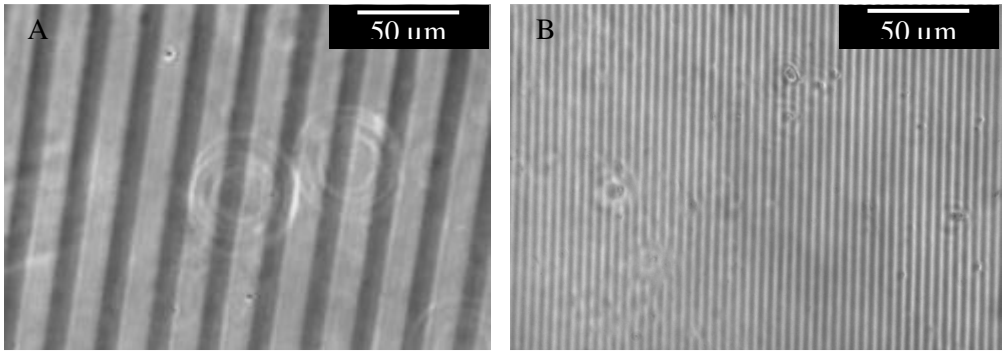

Figure 9: Bright-field images of PVA films in PBS made from PS moulds of (A) 10 µm and (B) 2 µm dimension aspect grating patterns after immersion in PBS for 7 days

6.2 Surface characterization of PVA tubes with patterned lumen

After it was established that PVA films could be patterned via solvent casting techniques, it was desired to see if the patterned film could be incorporated into a tube, an eventually as a vascular graft. Using glass rods as tubular moulds as previously described, intact tubes of 2 mm diameter could be made in this manner. However, grating patterns of prepared PVA tubes appeared diminished during the rolling and dipping process, as observed from SEM images of the 250 nm grating dimension sample. The poor pattern quality could be attributed to the method of annealing the rolled films by coating with PVA. During the initial vertical dipping of the wrapped film into a reservoir of PVA solution, fluid pressure and capillary action might have caused the PVA solution to travel up through the gap between the wrapped PVA film and the glass rod, causing loss of some pattern.

Improvements to the dipping method have to be made in future to preserve the micro- or nano-topography of the solvent-casted patterns. For instance, the ends of the tube may be clamped or sealed with a hydrophobic plug, such as silicone glue, such that solution may not contact with the inner tube lumen during the dipping procedure.

However, it was generally observed that, compared to grafts produced by directly dipping and coating of the glass rod with PVA solution, the lumen of grafts produced with wrapped PVA film were macroscopically smoother in appearance (Figure 10). Macroscopic roughness is generally undesired in vascular graft lumens, as the lumen roughness might likely cause turbulence and energy loss by friction in blood flow through the graft after implantation. This in turn increases the likelihood of thrombus formation, decreasing graft patency [97].

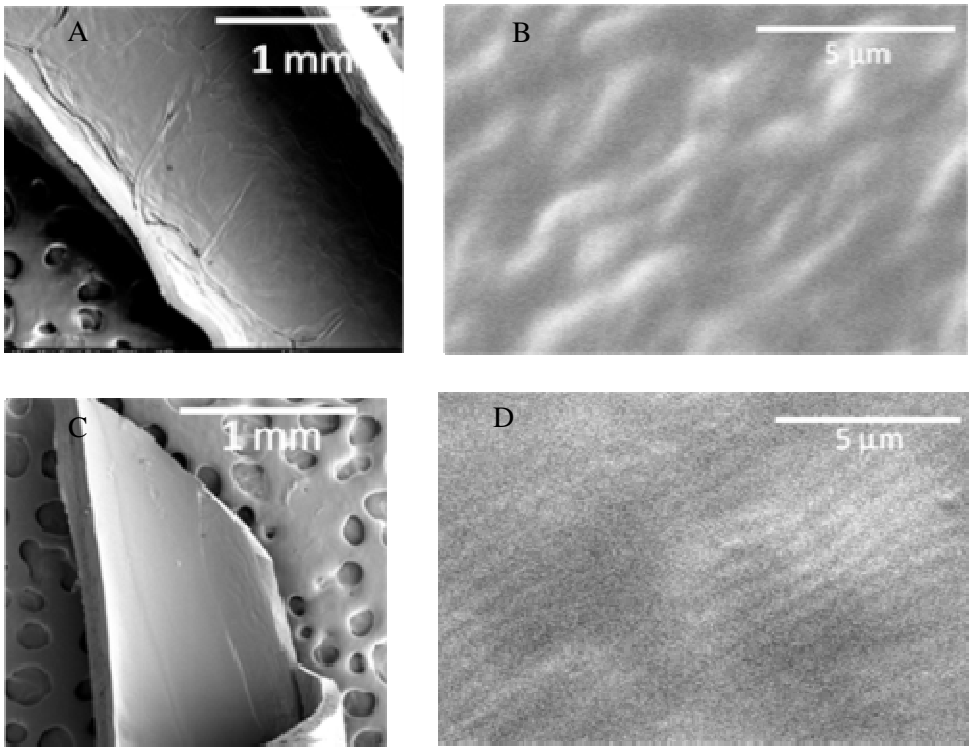

Figure 10: SEM images of PVA tube cross-sections produced by (A) direct dipping of PVA solution onto glass rods and (B) a close-up of the lumen surface topography and (C) wrapping of patterned film around glass rods followed by dipping, and (D) a close up of the lumen surface topography

6.3 Controlled release properties of PVA scaffolds

As the PVA tubes were prepared by a simultaneous evaporation and cross-linking process, PVA chains within the tube scaffold were more tightly packed and possessed a greater density of cross-linking compared to the polysaccharide scaffold. As such, it was necessary to investigate whether the PVA scaffold was permeable to macromolecules before the tubular scaffold's controlled

release properties could be investigated. Trypsin and BSA were chosen as model molecules for this experiment as their molecular weights were of similar order of magnitude to that of VEGF . In order to investigate the influence of charge on the molecule permeability, the molecules were also chosen on the basis that they expressed different charge polarities in physiological solution of pH 7.4.

It was observed that trypsin readily diffused across the PVA film, while the concentrations of BSA in both upper and lower chambers (Figure 1) remained relatively stable over the 48 hours, indicating no significant diffusion took place. Trypsin concentrations gradually equilibrated in both chambers over 48 hours, marked by a gradual decrease in the rate of change of trypsin quantity over time (Figure 11).

At this point, it was postulated that the negatively charged phosphate groups in the cross-linked PVA film created a high electrostatic energy barrier for which the negatively-charged BSA could not cross. However, the positively-charged trypsin, which was also nearly three times smaller in molecular weight, appeared to cross the PVA film membrane more easily, as there was no surmounting energy barrier to overcome for the trypsin to approach and cross the PVA membrane. This was also in agreement to Shalviri et al.'s work on the permeability of negatively charged polysaccharide membranes to variously charged and sized molecules [98], where the group showed that molecules of opposite charge to the membrane had a nearly five-fold increase in permeability compared to molecules of similar molecular weight but possessing the same charge polarity to the membrane.

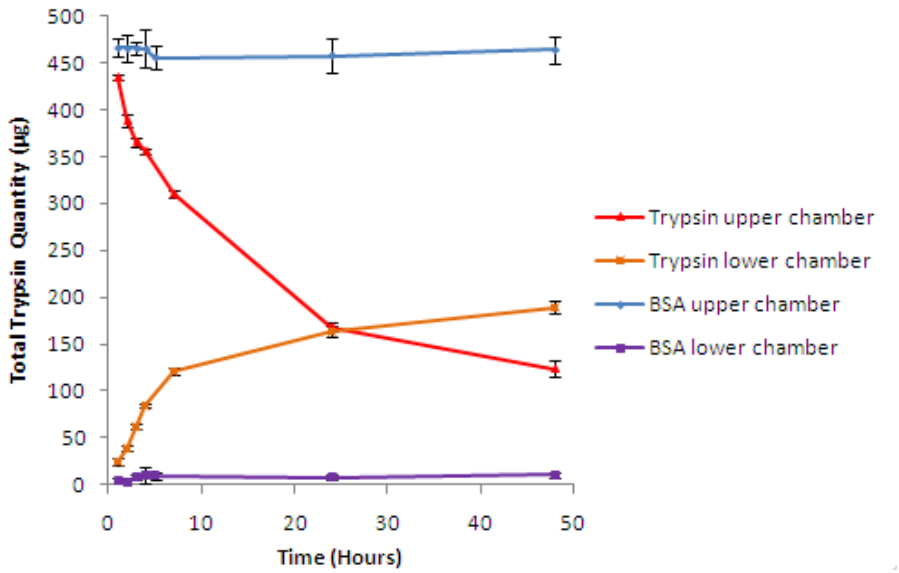

Figure 11: Graph of the concentrations of trypsin and BSA in the upper and lower chamber solutions taken during permeability assessment of the PVA membrane over time

Trypsin was thus selected over BSA as the model molecule to use for controlled release studies of the PVA-fiber composite tubular scaffold. With the presence of a high density of negative charges from phosphate groups within the cross-linked PVA, it was a point of contention as to whether tubular PVA scaffolds could also serve as steady release reservoirs of positively-charged protein, and eventually VEGF, over time. The encapsulation efficiency of trypsin was measured to be 88.0±0.8%, and thus the percentage released was normalized against the percentage of trypsin encapsulated.

With the previous VEGF controlled release data previously obtained, the polyanion solution composed of an alginate: heparin ratio of 9:1 was used for the controlled release of trypsin.

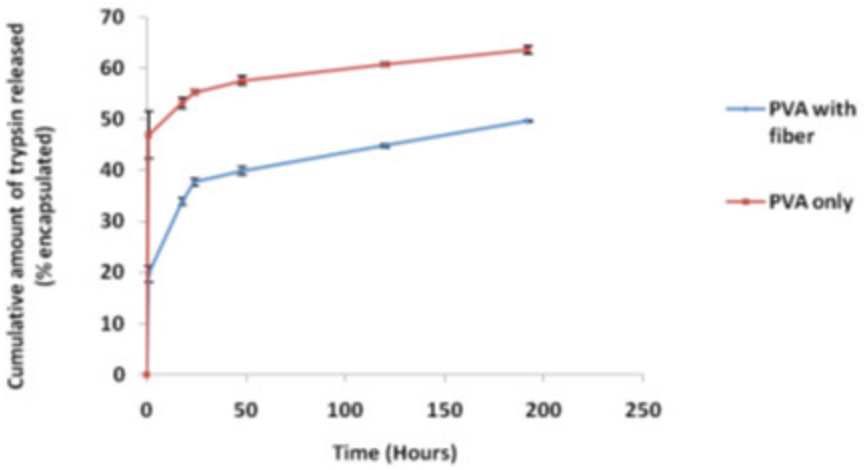

Figure 12: Graph of cumulative release of trypsin from PVA-fiber composite and PVA-only tubular scaffolds over a period of 8 days

Controlled release experiments performed with the two scaffold types showed that PVA-only tubes indeed displayed a prolonged release of trypsin over the experiment period of 8 days, despite the initial high burst release of over 45% (Figure 12). PVA-fiber composite tubes had a lower burst release rate than tubes composed of only PVA, the former having an initial burst release of less than half that of the latter in the first two hours. It could be inferred that the incorporation of PEC fibers into the PVA tubes could lower the initial rate of trypsin release, possibly as the protein was regulated in its diffusion by both the polyanion to which it had interacted in the PEC fibers during polyelectrolyte complexation, and the negative charges present in the cross-linked PVA scaffold.

6.4 Mechanical testing of PVA and PVA-fiber composites

While PVA is a relatively elastic material, PEC fibers have been known to be characteristically stiff [99,100], thus one primary concern that the incorporation fibers could compromise on the mechanical properties of the PVA-fiber tubular graft. As mentioned previously, a common factor associated with short-term patency of conventional grafts is their relative stiffness and low compliance compared to native tissue. The mechanical test was thus performed to investigate the

influence of PEC fiber, including the effect of the orientation of the fibers within the scaffold, on the mechanical properties of the PVA-fiber composite. This could thus determine a suitable fiber orientation to use in the composite tubular graft.

The elastic modulus of the composite E_c was measured from the tangential gradient of the graph segment between stress values of 0 to 49,050 N/m^2, as this range corresponds to native stresses which the vessels are subjected to in the body [33]. Tensile test results (Figure 13A) showed that the elastic modulus for samples with parallel PVA fibers was 4.2 x 10^5 N/m^2, greater than that of samples with perpendicular or no fibers, which was expected of composites under isostrain. In contrast, the PVA-fibers in perpendicular orientation, which were subjected to isostress, and the PVA samples were not significantly different from each other, and had approximate elastic moduli of 3.75 x 10^5 N/m^2.

The results obtained were in fact consistent with the known behaviour of anisotropic composites under stress. In the isostrain configuration of loading, the total load force experienced by the composite F_c is approximately the combined contribution of the PVA load force F_m and fiber load force F_f, as illustrated in equation (5.1), where σ is stress of the respective components, and A is the cross-sectional area of the respective components, perpendicular to the direction of stretch.

$$F_c = \sigma_c A_c = F_m + F_f = \sigma_m A_m + \sigma_f A_f \quad (5.1)$$

$$\varepsilon_c = \varepsilon_{pva} = \varepsilon_f \quad (5.2)$$

$$\sigma = \varepsilon E \quad (5.3)$$

In addition, the strain experienced by the composite and its components were the same, as they are stretched to the same degree, as outlined in equation (5.2). Given the general relationship between the stress, strain and elastic modulus of materials in equation (5.3), the resultant elastic modulus of the PVA-fiber composite under isostrain could be inferred from the abovementioned three equations to give equation (5.4).

$$E_c = E_{pva}\frac{A_{pva}}{A_c} + E_f\frac{A_f}{A_c} \qquad (5.4)$$

In contrast, for fibers and PVA under isostress, an approximately equal amount of stress was transmitted across both fiber and PVA during tensile testing, while the total elongation of the composite was the sum of the elongation of the two components, as both components were positioned in series to the tensile force. This can be surmised by equations (5.5) and (5.6), where L is the component of the length parallel to the direction of applied force. Hence, the relationship for the Elastic moduli under isostress is given by the equation (5.7).

$$\sigma_c = \sigma_{pva} = \sigma_f \qquad (5.5)$$

$$\varepsilon_c L_c = \varepsilon_{pva} L_{pva} + \varepsilon_f L_f \qquad (5.6)$$

$$\frac{1}{E_c} = \frac{1}{E_{pva}}\left(\frac{L_{pva}}{L_c}\right) + \frac{1}{E_f}\left(\frac{L_f}{L_c}\right) \qquad (5.7)$$

Comparing the two relationships, the fiber, with its relatively high elastic modulus, contributed more significantly to the overall elastic modulus of the composite under isostrain conditions compared to isostress. In contrast, the stiffness of the fiber has a diminished influence when

orientated perpendicular to the direction of strain, resulting in no distinct difference in stiffness from the PVA-only samples.

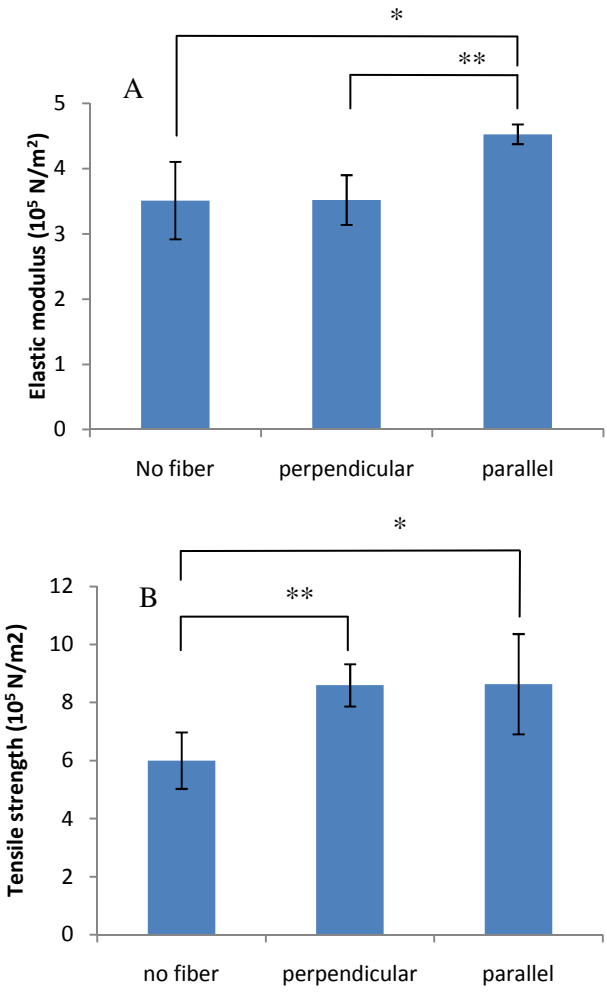

Figure 13: The (A) elastic modulus and (B) tensile strength of samples obtained from the tensile test experiment on PVA-only scaffold, PVA-fiber composite samples with fibers in perpendicular and parallel orientation. (*: p<0.1, **: p<0.05)

Chandran et al. reported the average elastic modulus of arteries to be 4.55 x 10^5 N/m^2 [101], which approximated closely to the measured elastic modulus of the PVA-fiber scaffold with fibers in parallel orientation. However, arterial elastic moduli have been shown to vary greatly under different conditions. For example, several groups had shown that carotid arteries become stiffer with age [34, 102]. The elastic modulus also varies with the artery anatomical location. For example, measurements of the carotid artery range at 3.0 – 8.0 x 10^5 N/m^2, but a much higher

stiffness has been measured from the femoral artery, at 12 - 40 x 10^5 N/m^2 [103]. As such, should the PVA-fiber composite be used as a graft, the elastic modulus of the graft can be varied by changing the ratio of fiber to PVA, as well as angle of fiber orientation to the graft axis.

Fibers in parallel to the direction of strain were observed to fracture early at low strain, hence the short fiber fragments were thought to have limited contribution to the load bearing thereafter, while strength contribution from fibers orientated perpendicular to the direction of stress was thought to be low as well. However, the tensile strength of both composite sample types were observed to be higher than that of PVA samples with no fibers incorporated (6.0 x 10^5 N/m^2), and both composite stresses measured about 8.5 x 10^5 N/m^2, regardless of the fiber orientation (Figure 12B). Interfacial bonding between the PVA and fibers was one plausible explanation for the higher tensile strength in the composites [104,105], where the presence of electrostatic or Van der Waal's forces of attraction between fibers and the surrounding PVA at their interface provided the transfer of load from the PVA to the fibers. Although the maximum tensile stress of all three sample configurations were still lower than that of native arteries, it is highly unlikely that such tensile stress values would be reached under physiological conditions [33,34], where the maximal active stress values of arteries were reported to be in the range of 1.5 x 10^5N/m^2 [106,107].

6.5 Cell morphology studies of HUVEC cultured on PVA films

As mentioned previously in chapter 3, PVA has generally been considered as an unfavourable material for cell adhesion due to its chemical structure, which contributes to its strongly hydrophilic nature. HUVEC cells seeded on PVA scaffolds of grating patterns with dimensions 2 μm and 250 nm were observed to display greater cell density and number compared to the PVA control with no grating patterns. This was an indication that the influence of topography could not be ignored over surface chemistry, although current mechanisms of topography on cell behaviour remain unclear.

Between the two dimensions of gratings, 250 nm had a visibly higher number of cells attached compared to the 2 µm film samples. Moreover, cells appeared to be spread out more on the PVA films of dimensions 250 nm compared to the cells on films of dimensions 2 µm.

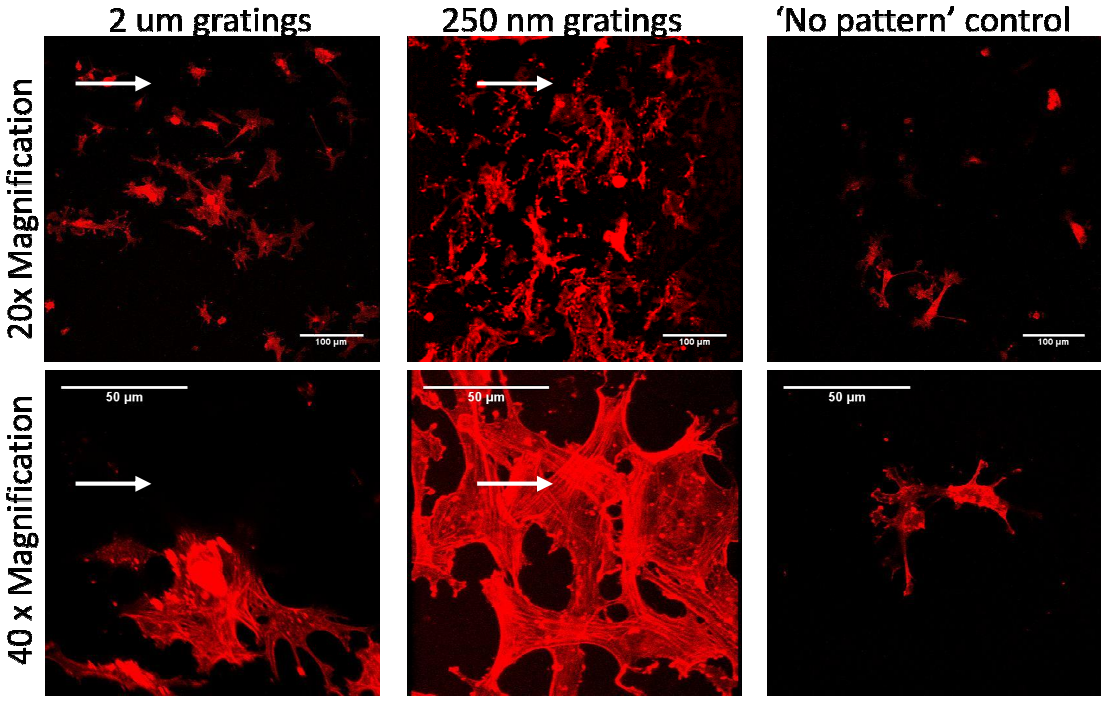

Figure 14: Fluorescent images of HUVEC cells seeded on patterned PVA scaffolds of grating pattern dimensions 2 µm, 250 nm and blank controls with no pattern. Cells were stained for their actin filament structure with phalloidin-TRITC. The direction of the gratings is indicated by the arrows in the images.

One of the possible reasons could be the influence of topography on protein adsorption on the PVA surface, either of proteins from the medium or ECM proteins synthesized and secreted by the cells during culture, specifically fibronectin for endothelial cells [124]. Generally, adhesion of anchorage-dependent mammalian cells to a substrate surface follows the sequence of protein adsorption to the surface, cell-protein contact, followed by cell attachment and spreading. Hence the initial step of protein adsorption is crucial for cell adhesion to a substrate surface. For example, fibronectin, an oblate ellipsoid-like, high molecular weight glycoprotein component of the ECM that binds to integrins on the cell surface to promote cell adhesion, tends to adopt a more expanded,

often linear configuration on flat, hydrophilic surfaces [108]. However, fibronectin better retains its native globular shape when adsorbed on surfaces with high curvatures, such as nanoparticles or ridges of the nano-scale range [109]. As such, binding sites of the fibronectin for cell attachment on the patterned substrate surface become available and thus could potentially improve cell attachment. However, such a hypothesis was not verified in this experiment, which could be done in future studies by checking the presence or distribution pattern of protein deposition on the gratings.

Although endothelial cells did not appear to align in the direction of the gratings, studies by Uttayarat et al. [62] and Biela et al. [58] showed that endothelial cells also did not display significant elongation and alignment under static conditions, doing so only when the cell cultures were subjected to shear flow conditions.

The cell study on patterned and non-patterned PVA films was fairly preliminary and no quantifiable data was obtained at this point of time. Nevertheless, it was still promising to note that there was a visual difference in cell behaviour towards the three different surface topographies of PVA, notably of which it seemed the presence of micro- and nano- grating topography appeared to enhance cell attachment to the scaffold.

CHAPTER 7

Conclusion

Due to the inherent problems associated with fabricating suitable small-diameter synthetic vascular grafts, a long-term solution has yet to be found for treatment of lower limb vascular diseases, many of which involve arteries of less than 6 mm in diameter. Two solutions proposed are the functionalization of the graft by incorporating a source of biomolecular cues to enhance vascular tissue regeneration and the endothelialisation of the graft lumen to maximise blood compatibility. In this study, two graft material candidates, PVA and pullulan-dextran polysaccharides, have been investigated to improve their functionality as bioactive scaffolds. The two materials had previously been investigated as vascular grafts in experiments. Although both types of materials were biocompatible and showed short-term patency, both materials were relatively inert, and did not contribute actively to tissue regeneration processes.

From the controlled release experiments, it has been demonstrated that the combination of PEC fibers with PVA or polysaccharide scaffolds improved the resulting composite scaffolds' ability to produce a sustained release of proteins. With regards to the polysaccharide-fiber composite scaffold, a sustained release of BSA and VEGF was observed, with the composite scaffold exhibiting a relatively lower burst release compared to the release from PEC fibers only.

The PVA scaffold was shown in this study to be impermeable to the negatively charged protein BSA, but permeable to the positively-charged protein Trypsin, due to the scaffold's high polymer density due to the solvent casting process. PVA-fiber composite scaffold showed a sustained release of Trypsin and a relatively lower burst release compared to the release profile of the PVA-only scaffold, demonstrating that the incorporation of PEC fibers had improved the sustained release of Trypsin over time in the PVA-fiber composite scaffold.

This study has also demonstrated that a simultaneous solvent-casting and cross-linking fabrication method can be used for the production of patterned PVA films, with the patterns being successfully retained when immersed in physiological solution. This method of pattern production is an advantage over other current methods such as electron beam lithography, polymer demixing and chemical etching [61], as the method allows the replication patterns on the micro- and nano-scale, with the ability to replicate large surface areas of the pattern simultaneously. Furthermore, no organic solvent is employed, eliminating the possibility of cytotoxic effects that may be caused by residual solvents. With the current method of producing small-diameter PVA tubes with patterned lumens, the surface macro-structure can be controlled.

Endothelial cell adhesion studies on micro- and nano-patterned PVA films, fabricated using the abovementioned method, have also shown improved endothelial cell adhesion of HUVECs on patterned surfaces compared to non-patterned PVA surfaces. In particular, of the two grating dimension patterns, surfaces of PVA films with gratings of dimensions 250 nm appeared to demonstrate better cell adhesion than that on gratings of dimensions 2 μm. The demonstration of improvement of endothelial cell adhesion to patterned PVA surfaces is a promising result that could lead to the use of patterned surfaces in PVA vascular graft lumens to enhance endothelial cell adhesion.

Fibroblast cell adhesion studies conducted on the polysaccharide-PEC scaffold showed two different types of cell behaviour on each scaffold component. Fibroblast cells on the polysaccharide surface assumed a spherical morphology with poor cell adhesion. This was favourable as a graft material surface with low fibroblast adhesion tends to discourage intimal hyperplasia or stenosis formation within the graft lumen. On the other hand, although cell adhesion to the embedded fibers was also poor, cells appeared to align to the long axis of the fibers, showing that the fibers displayed some degree of contact guidance to the cells.

The effect of the incorporation of PEC fibers on the overall mechanical properties of PVA-fiber composites was also investigated in this study. It was shown that the incorporation of fibers not only improved the elastic modulus of the PVA-fiber scaffold over the PVA-only scaffold, but also increased its maximum tensile strength.

CHAPTER 8

Future Work

Both scaffolds have the advantage of being fabricated completely in aqueous solutions at physiological temperatures. As no high temperature treatment and organic solvents were involved in the fabrication processes, biological molecules such as growth factors could be incorporated into the scaffold during the fabrication process. This was successfully demonstrated in the controlled release experiments performed, with the results as described above.

An advantage of such a method of protein incorporation within PEC fibers during the scaffold fabrication process is the ability to control the spatial distribution within the scaffold of the protein encapsulated. For example, endothelial cells are known to be chemotactic, showing propensity to migrate in the direction of increasing concentrations of VEGF [110]. It has been of general interest to develop a tubular graft that can produce a gradient of growth factor to direct and promote endothelial cell growth in vascular grafts [111], which can be achieved by localizing fibers encapsulating VEGF towards the middle of the scaffold during graft fabrication. In this manner, a bi-directional gradient of VEGF can be established as VEGF is continuously released by the fiber and diffuses along the length of the tube. As endothelialisation of implanted vascular grafts is often a slow and incomplete process, graft materials are left exposed to blood flow for prolonged periods of time and are susceptible to thrombogenicity. A gradient of growth factor in the graft could thus shorten the time required for re-endothelialisation, improving graft patency.

However, further studies have to be carried out in characterizing the scaffolds as sustained release reservoirs for growth factors. In the case of the polysaccharide-fiber scaffold, a controlled and sustained release of BSA from the polysaccharide-fiber scaffold has been shown. While controlled release of VEGF from the scaffold has been demonstrated, a longer period of assessment should

be done in order to obtain a more comprehensive release profile of VEGF from the polysaccharide scaffold.

In addition, although the released growth factor can be detected by ELISA indicating that the VEGF peptide is likely still intact, additional bioactivity studies of the released VEGF have to be performed to ensure that both encapsulated and released VEGF have not denatured and still retain their bioactivity. The bioactivity of VEGF could be evaluated in vitro by determining the proliferative capacity of an endothelial cell line after VEGF treatment. For VEGF released in solution, supernatant of the release solution could be collected and incubated with an in vitro culture of endothelial cells. VEGF retained within the PEC fiber could be obtained in solution by extracting the PEC fiber from the gel and performing a digestion of the fiber using chitosanase and alginase. Incubation of cells with medium containing a prepared concentration of VEGF and medium without VEGF would serve as positive and negative experiment controls respectively. Cell proliferation could be quantified at the end of the incubation period by performing by cell count using a haemocytometer. By quantifying the proliferation rates of in-vitro HUVEC cultures, the rate of proliferation would serve as an indicator to whether VEGF, both in solution and within the PEC fiber, still remains bioactive.

While permeability and controlled release experiments with trypsin as the model molecule have shown that PVA tubular scaffolds can act as controlled release reservoirs as well, trypsin has been found to possess autolytic activities [112], thus altering the molecular weight of the enzyme by introducing peptide fragments and rendering the permeability experiment inaccurate in terms of determining the molecular weight of protein that may pass through the PVA membrane. It is thus necessary to repeat the experiments with an alternative protein that is stable under such experimental conditions. Positively charged proteins such as lysozyme, cationic trypsinogen and cytochrome C [113,114] can be considered as model proteins in place of VEGF to assess

permeability and controlled release properties, which would otherwise be too costly to be used in such preliminary experiments. Eventually, after the controlled release capability of the PVA-fiber tubular graft has been ascertained, release properties of the graft with VEGF may be carried out.

Cell adhesion studies on the polysaccharide-fiber scaffold, particularly on the observed contact guidance of fibroblasts by the PEC fibers in the scaffold, could be further investigated. PEC fibers could potentially be used to guide the growth of cells and hence regeneration of tissue within the vascular graft. In particular, fibers could potentially guide the growth and alignment of smooth muscle cells in the graft, providing a possible approach to regenerating the tunica media of the artery. Smooth muscle cells are typically arranged in a concentric, helical manner within the vessel tunica media [116]. and the structure and alignment of smooth muscles cells in native vessels are crucial in providing active tension in muscle contraction, as well as increasing circumferential stiffness to resist distension [117].

ECM proteins may be incorporated into PEC fibers to improve their cell adhesion properties, an application that could be investigated in future studies. In a recently published study on liver tissue regeneration by Tai et al., hepatocytes were successfully cultured on PEC fibers incorporated with various ECM molecules native to liver tissue [115], showing the possibility of modulating cell adhesion properties of PEC fibers with this method. Further studies can be performed to assess the improvement of smooth muscle cell adhesion to PEC fibers incorporated with native extracellular matrix proteins such as elastin. Fibers may be embedded in a continuously drawn, helical manner around the tubular graft to mimic the orientation of smooth muscle cells within native vessels. By controlling the orientation of the fibers within the scaffold and type of ECM molecules incorporated, it would be possible to modulate the tissue regenerative capabilities of the composite graft.

Endothelial cell adhesion experiments performed on the patterned PVA films will have to be repeated for consistency, and quantification of the proliferation as well as cell spreading can be performed to provide a clearer perspective on the degree of influence the patterned films have on the cells. In addition, protein deposition assays could be done to verify the hypothesis that there was preferential adsorption of proteins to curvatures on the nano- or micr-gratings, that resulted in better cell adhesion to the gratings. This could be carried out by incubating FITC-conjugated fibronectin with PVA films, and thereafter observing the protein distribution pattern under fluorescence microscopy. As HUVECs have been known to secrete fibronectin in culture [124], cell-seeded PVA films could be de-cellularized after a period of culture, and the films with the remaining protein deposited can be immunostained for fibronectin, which can then be visualized by fluorescence microscopy.

As studies by Uttayarat et al. [62] and Biela et al. [58] have shown, cells are more likely to exhibit alignment and migration tendencies under native vessel flow conditions. Hence, patterned tubes seeded with endothelial cells in their lumen can be subjected to flow conditions using a bioreactor, and thereafter assessed for endothelial cell alignment against cell-seeded tubes cultured under static conditions. Migration of endothelial cells would be better assessed with real-time imaging of the cultures on patterned PVA films, using a heated flow chamber mounted on a microscope stage, as tubular scaffolds are opaque and would pose problems should real-time viewing of the cultures in the patterned lumen be desired.

Further to the improved mechanical properties observed in the PVA-fiber scaffold, additional studies on the moderation of the fiber-to-PVA ratio as well as fiber orientation within the scaffold could be done to expand the indications of the PVA-fiber scaffold to different anatomical sites and patient age groups, where vessel mechanical properties would vary significantly.

Another important mechanical property to consider is the compliance of the graft, which is defined as the degree of distension of the vessel or graft in response to changes in blood pressure [118], and should match closely to that of the host artery. To investigate vessel compliance, a mechanical setup comprising of a pressure gauge fitted on one end of the graft to be measured and an injector system secured to the other can be utilised. By taking measurements of the graft volume expansion between 120 mmHg and 80 mmHg, which are the systolic and diastolic pressures experienced by native arteries, the compliance of the graft can be assessed [119].

Finally, implanted grafts would inevitably undergo a multitude of interactions in a complex physiological environment, including interactions with blood serum proteins, inflammatory cytokines [120] and a variety of tissue and cell types. As in-vitro experiments can only provide limited information on how the grafts might perform after implantation, in-vivo experiments will ultimately have to be carried out on grafts. Information that can be obtained would be the degree of tissue regeneration the graft can support, namely the induction of spontaneous endothelialisation, or migration and alignment of smooth muscle cells. Patency of grafts can also be assessed, by looking into the susceptibility of the graft lumen to thrombogenesis, or presence of anastomotic aneurysm formation due to vessel fatigue at the anastomosis sites [121].

Although the results presented here are preliminary and further studies have yet to be done to create a more detailed and defined characterization of the scaffolds as vascular grafts, PVA and polysaccharide scaffolds in this study have shown promise as candidates for vascular graft tissue regeneration, in terms of their ability to perform controlled release of biologics, as well as the presence of topographical cues that might provide the necessary cell guidance cues for successful tissue regeneration.

BIBLIOGRAPHY

1. Mitchell RN. Graft vascular disease: immune response meets the vessel wall. Annual Review of Pathology. 4, pp.19-47. 2009
2. Lloyd-Jones D, Adams R, Carnethon M, De Simone G, Ferguson TB, Flegal K, Heart disease and stroke statistics--2009 update: a report from the American Heart Association Statistics Committee and Stroke Statistics Subcommittee. *Circulation*. 119, pp.21-181. 2009
3. Singhealth Groups 2010, Singapore, accessed 25/06/2010 <http://www.singhealth.com.sg/PatientCare/ConditionsAndTreatments/Pages/Peripheral-Arterial-Disease.aspx>
4. Koh WP, Loh JKX, Phang J, Peripheral Arterial Disease among Diabetic Patients in the Community- the National Healthcare Group Polyclinics (NHGP) Study, National University of Singapore, Singapore, accessed 25/06/2010 < http://www.med.nus.edu.sg/cof/0024-Koh__Woon_Puay43189.pdf>
5. McCollum PT, Walker MA, The Choice Between Limb Salvage and Amputation: Major Limb Amputation for End-Stage Peripheral Vascular Disease: Level Selection and Alternative Options. Chapter 2C, Atlas of Limb Prosthetics: Surgical, Prosthetic, and Rehabilitation Principles. Rosemont, IL, American Academy of Orthopedic Surgeons, ed. 2, 2002.
6. De Felice M, Gallo P, Masotti G. Current therapy of peripheral obstructive arterial disease. The non-surgical approach. Angiology. 41, pp.1-11. 1990
7. Hiatt WR, Medical treatment of peripheral arterial disease and intermediate claudication. New England Journal of Medicine, 344, pp.1608-1621 2001
8. Peng PD, D'Amelio LF, Greco RS, Biologic Properties of Venous Access Devices,Vascular Access: Principles and Practice, Lippincott Williams & Wilkins, 2009
9. Fowkes F, Leng GC, Bypass surgery for chronic lower limb ischaemia. The Cochrane Library. 2, pp.1-42, 2008
10. Kahn ML, Bennett JS, Brass LR, Poncz M, Platelet Membrane Proteins and Their Disorders, Blood: Principles and Practice of Hematology, Volume 1, Lippincott Williams & Wilkins, 2003
11. Cull DL, Langan EM, Gray BH, Johnson B, Taylor SM, Open versus endovascular intervention for critical limb ischemia: a population-based study. Journal of the American College of Surgeons. 210, pp.555-61, 561-3, 2010
12. Lipsitz EC, Berdejo GL, Rationale and benefits of surveillance after percutaneous transluminal angioplasty after stenting of iliac and femoral arteries. Noninvasive Peripheral Arterial Diagnosis. Springer, 2010
13. Woods TC, Marks AR, Drug-eluting stents, Annual Review of Medicine. 55 pp.169–78, 2004
14. Daemen J, Serruys PW. Drug-eluting stent update 2007: part I. A survey of current and future generation drug-eluting stents: meaningful advances or more of the same? Circulation. 116, pp.316-28, 2007
15. Ahn SS, Ro KM, Chapter 24 - Peripheral Atherectomy, Vascular surgery: principles and practice, Marcel Dekker, Inc., 2004
16. Goodney PP, Beck AW, Nagle J, Welch HG, Zwolak RM, National trends in lower extremity bypass surgery, endovascular interventions, and major amputations. Journal of Vascular Surgery, 50, pp.54-60, 2009

17. Salacinski HJ, Goldner S, Giudiceandrea A, Hamilton G, Seifalian AM, Edwards A, Carson RJ. The mechanical behavior of vascular grafts: a review. Journal of Biomaterial Applications.15, pp.241-78, 2001
18. Lamm P, Juchem G, Milz S, Schuffenhauer M, Reichart B. Autologous endothelialized vein allograft: a solution in the search for small-caliber grafts in coronary artery bypass graft operations. Circulation. 18, pp. I108-14, 2001
19. Beard JD, Which is the best revascularization for critical limb ischemia: Endovascular or open surgery?, Journal of Vascular Surgery 48, pp.11S-16S, 2008
20. Sarkar S, Schmitz-Rixen T, Hamilton G, Seifalian AM. Achieving the ideal properties for vascular bypass grafts using a tissue engineered approach: a review. Medical & Biological Engineering & Computing, 45, pp. 327-36, 2007
21. Twine CP, McLain AD. Graft type for femoro-popliteal bypass surgery. Cochrane Database Systematic Reviews 12, CD001487. 2010
22. Cummings CL, Properties of engineered vascular constructs made from collagen, fibrin, and collagen-fibrin mixtures. Biomaterials, 25, pp.3699–3706, 2004
23. Swartz DD, Russell JA, Andreadis ST, Engineering of fibrin-based functional and implantable small-diameter blood vessels. Americal Journal of Physiology. Heart Circulation Physiology, 288, ppH1451–60, 2005
24. Hirai J, Matsuda T, Venous reconstruction using hybrid vascular tissue composed of vascular cells and collagen—tissue regeneration process. Cell Transplant, 5, pp.93–105, 1996
25. Patel A, Fine B, Sandig M, Mequanint K. Elastin biosynthesis: The missing link in tissue-engineered blood vessels. Cardiovascular Research. 71, pp.40-9, 2006
26. L'Heureux N, Dusserre N, Marini A, Garrido S, de la Fuente L, McAllister T. Technology insight: the evolution of tissue-engineered vascular grafts--from research to clinical practice. Nature Clinical Practice Cardiovascular Medicine. 4, pp.389-95, 2007
27. L'Heureux N, Pâquet S, Labbé R, Germain L, Auger FA. A completely biological tissue-engineered human blood vessel. FASEB Journal,12, pp.47-56, 1998
28. Suvilian S, Brockbank KGM, Small-diameter vascular grafts, Principles of Tissue Engineering, Edn. 2, Academic Press, 2002
29. Sarkar S, Sales KM, Hamilton G, Seifalian AM. Addressing thrombogenicity in vascular graft construction. Journal of Biomedical Materials Research B. Applied Biomaterials. 82, pp.100-8, 2007
30. Kader KN, Akella R, Ziats NP, Lakey LA, Harasaki H, Ranieri JP, Bellamkonda RV. eNOS-overexpressing endothelial cells inhibit platelet aggregation and smooth muscle cell proliferation in vitro. Tissue Engineering, 6, pp.241-51, 2000
31. Llanos GR, Sefton MV. Does polyethylene oxide possess a low thrombogenicity? Journal of Biomaterials Science. Polymer Edition, 4, pp.381-400, 1993
32. Stewart SF, Lyman DJ, Predicting the compliance of small diameter vascular grafts from uniaxial tensile tests. Journal of Biomechanics, 23, pp.629-37, 1990
33. Tseders EE, Purinya BA, The mechanical properties of human blood vessels relative to their location, Mechanics of Composite Materials, 11, pp. 271-275, 1975
34. Khamin NS, The strength properties of the human iliac and carotid arteries and their changes with age, Mechanics of Composite Materials, 14, pp.715-18, 1978

35. Berni GA et al., Changing Etiology of Anastomotic Aneurysms, Vascular and Endovascular Surgery, 16, pp.76-85, 1982
36. Panasche, P.E., Kinley, F.G., et al.: Consideration of suture line stresses in the selection of synthetic grafts for implantation. Journal of Biomechanics, 253, 1973.
37. Matsumoto H, Hasegawa T, Fuse K, Yamamoto M, Saigusa M, A new vascular prosthesis for a small caliber artery. Surgery, 74, pp.519–523, 1973
38. Zorlutuna P, Hasirci N, Hasirci V, Nanopatterned collagen tubes for vascular tissue engineering. Journal of Tissue Engineering and Regenerative Medicine. 2, pp.373-7, 2008
39. Greisler HP, Tattersall CW, Henderson SC, Cabusao EA, Garfield JD, Kim DU. Polypropylene small-diameter vascular grafts. Journal of Biomedical Materials Research. 26, pp.1383-94, 1992
40. Hasan CM, Peppas NA, Structure and Morphology of Freeze/Thawed PVA Hydrogels, Macromolecules, 33, pp.2472-2479, 2000
41. Yang X. et al., Effects of PVA, agar contents, and irradiation doses on properties of PVA/ws-chitosan/glycerol hydrogels made by g-irradiation followed by freeze-thawing, Radiation Physics and Chemistry 77, pp.954– 960, 2008
42. Mallapragada, McCarty-Schroeder,PVA as a drug delivery carrier, Handbook of pharmaceutical controlled release technology, CRC Press, 2000
43. Gendler E, Gendler S, Nimni ME, Toxic reactions evoked by glutaraldehyde-fixed pericardium and cardiac valve tissue bioprosthesis. Journal of Biomedical Materials Research 18, pp.727–36, 1984
44. Chaouat M, le Visage C, Baille WE, Escoubet B, Chaubet F; Alexandru MM, Letourneur D, A Novel Cross-linked Poly(vinyl alcohol) (PVA) for Vascular Grafts, Advanced Functional Materials.18, pp. 2855-2861, 2008
45. Fauvel-Lafeve F, Microfibrils from the arterial subendothelium. In Rev Cytol 188, pp.1–40, 1999
46. Berglund JD, Nerem RM, Sambanis A, Incorporation of intact elastin scaffolds in tissue-engineered collagen-based vascular grafts. Tissue Engineering, 10, pp.1526–1535, 2004
47. Simionescu DT, Lu Q, Song Y, Lee JS, Rosenbalm TN, Kelley C, Biocompatibility and remodeling potential of pure arterial elastin and collagen scaffolds. Biomaterials, 27, pp.702–713, 2006
48. Sell SA, McClure MJ, Barnes CP, Knapp DC, Walpoth BH, Simpson DG, Bowlin GL. Electrospun polydioxanone-elastin blends: potential for bioresorbable vascular grafts. Biomedical Materials 1, pp.72-80, 2006
49. Autissier A, Letourneur D, Le Visage C. Pullulan-based hydrogel for smooth muscle cell culture. Journal of Biomedical Materials Research A, 82, pp.336-42, 2007
50. Chaouat M, Le Visage C, Autissier A, Chaubet F, Letourneur D, The evaluation of a small-diameter polysaccharide-based arterial graft in rats. Biomaterials. 27, pp.5546-53, 2006
51. Thébaud NB, Pierron D, Bareille R, Le Visage C, Letourneur D, Bordenave L. Human endothelial progenitor cell attachment to polysaccharide-based hydrogels: a pre-requisite for vascular tissue engineering. Journal of Materials Science. Materials in Medicine, 18, pp.339-45, 2007
52. Duffy TC, Critical role of the vascular endothelial cell in health and disease: a review article, Journal of Veterinary Emergency and Critical Care, 14, pp.84 – 99, 2004

53. Kakou A, Louis H, Cattan V, Lacolley P, Thornton SN, Correlation between arterial mechanical properties, vascular biomaterial and tissue engineering. Clin Hemorheol Microcirc. 37, pp.71-5, 2007
54. Bhat VD, Klitzman B, Koger K, Truskey GA, Reichert WM, Improving endothelial cell adhesion to vascular graft surfaces: clinical need and strategies, J Biomater Sci Polym Ed, 9, pp.1117-35, 1998
55. van Wachem PB, Stronck JW, Koers-Zuideveld R, Dijk F, Wildevuur CR, Vacuum cell seeding: a new method for the fast application of an evenly distributed cell layer on porous vascular grafts. Biomaterials, 11, pp.602-6, 1990
56. Villalona GA, Udelsman B, Duncan DR, McGillicuddy E, Sawh-Martinez RF, Hibino N, Painter C, Mirensky T, Erickson B, Shinoka T, Breuer CK. Cell-seeding techniques in vascular tissue engineering. Tissue Engineering Part B Review,16, pp.341-50, 2010
57. Zorlutuna P, Rong Z, Vadgama P, Hasirci V, Influence of nanopatterns on endothelial cell adhesion: Enhanced cell retention under shear stress. Acta Biomater. 5, pp.2451-9, 2009
58. Biela SA, Su Y, Spatz JP, Kemkemer R. Different sensitivity of human endothelial cells, smooth muscle cells and fibroblasts to topography in the nano-micro range. Acta Biomater. 5, pp.2460-6, 2009
59. Uttayarat, P, Lelkes, Peter I, Composto, Russell J, Effect of Nano-to Micro-Scale Surface Topography on the Orientation of Endothelial Cells, MRS Proceedings Volume 845. 2004 Fall Meeting Symposium AA, Nanoscale Materials Science in Biology and Medicine
60. Bettinger CJ, Langer R, Borenstein JT. Engineering substrate topography at the micro- and nanoscale to control cell function. Angewandte Chemie International Edition English, 48, pp.5406-15, 2009
61. Ranjan A, Webster TJ. Increased endothelial cell adhesion and elongation on micron-patterned nano-rough poly(dimethylsiloxane) films, Nanotechnology. 20, pp.305102, 2009
62. Uttayarat P, Chen M, Li M, Allen FD, Composto RJ, Lelkes PI, Microtopography and flow modulate the direction of endothelial cell migration. Am J Physiol Heart Circ Physiol. 294, pp.H1027-35. 2008
63. Katsumi A, Orr AW, Tzima E, Schwartz MA. Integrins in mechanotransduction.. Journal of Biological Chemistry, 279, pp.12001–12004, 2004
64. Lamalice L, Le Boeuf F, Huot J, Endothelial cell migration during angiogenesis. Circulation Research, 100, pp.782-94, 2007
65. Sander EE, ten Klooster JP, van Delft S, van der kammen RA, Collard JG. Rac downregulates Rho activity: reciprocal balance between both GTPases determines cellular morphology and migratory behavior. J Cell Biol.147, pp.1009 –1022, 1999
66. Inoue M, Hager JH, Ferrara N, Gerber HP, Hanahan D. VEGF-A has a critical, nonredundant role in angiogenic switching and pancreatic beta cell carcinogenesis. Cancer Cell, 1, pp.193-202, 2002
67. Carmeliet P, Ferreira V, Breier G, et al: Abnormal blood vessel development and lethality in embryos lacking a single VEGF allele. Nature, 380 pp.435-439, 1996
68. Ferrara N, Vascular endothelial growth factor. European Journal of Cancer, 32A, pp.2413-2422, 1996
69. Ferrara N, Role of vascular endothelial growth factor in regulation of physiological angiogenesis, American Journal of Physiology. Cell Physiology 280, pp.1358-1366, 2001

70. Hicklin DJ, Ellis LM, Role of the vascular endothelial growth factor pathway in tumor growth and angiogenesis. Journal of Clinical Oncology, 23, pp.1011-27, 2005
71. Elisa Lappi-Blanco, Angiogenesis, apoptosis and re-epithelialization at the foci of recent injury in usual interstitial pneumonia and bronchiolitis obliterans organizing pneumonia, Academic Dissertation , Faculty of Medicine, University of Oulu, 2003
72. Grunstein J, Masbad JJ, Hickley R, Giordano F, and Johnson RS. Isoforms of vascular endothelial growth factor act in a coordinated fashion to recruit and expand tumor vasculature. Molecular Cell Biology 20, pp.7282–7291, 2000
73. Cheng SY, Nagane M, Huang HS, and Cavenee WK. Intracerebral tumor-associated hemorrhage caused by overexpression of the vascular endothelial growth factor isoforms VEGF121 and VEGF165 but not VEGF189. Proc Natl Acad Sci USA, 94, pp.12081–12087, 1997
74. Gerhardt H, Golding M, Fruttiger M, Ruhrberg C, Lundkvist A, Abramsson A, Jeltsch M, Mitchell C, Alitalo K, Shima D, Betsholtz C. VEGF guides angiogenic sprouting utilizing endothelial tip cell filopodia. Journal of Cellular Biology. 161, pp.1163-77, 2003
75. De la Riva B, Nowak C, Sánchez E, Hernández A, Schulz-Siegmund M, Pec MK, Delgado A, Evora C. VEGF-controlled release within a bone defect from alginate/chitosan/PLA-H scaffolds. Eur J Pharm Biopharm. 73, pp.50-8, 2009
76. Elcin AE, Elcin YM. Localized angiogenesis induced by human vascular endothelial growth factor-activated PLGA sponge. Tissue Engineering. 12, pp.959-68, 2006
77. Lee KY, Peters MC, Anderson KW, Mooney DJ. Controlled growth factor release from synthetic extracellular matrices. Nature. 408, pp.998-1000, 2000
78. Nillesen ST, Geutjes PJ, Wismans R, Schalkwijk J, Daamen WF, van Kuppevelt TH. Increased angiogenesis and blood vessel maturation in acellular collagen-heparin scaffolds containing both FGF2 and VEGF. Biomaterials, 28, pp.1123-31, 2006
79. Ishii Y, Kronengold RT, Virmani R, Rivera EA, Goldman SM, Prechtel EJ, Schuessler RB, Damiano RJ Jr. Novel bioengineered small caliber vascular graft with excellent one-month patency. Annals of Thoracic Surgery, 83, pp.517-25, 2006
80. Liao IC, Wan AC, Yim EK, Leong KW. Controlled release from fibers of polyelectrolyte complexes. Journal of Controlled Release, 104, pp.347-58, 2005
81. Yim EK, Liao IC, Leong KW. Tissue compatibility of interfacial polyelectrolyte complexation fibrous scaffold: evaluation of blood compatibility and biocompatibility. Tissue Eng. 13, pp.423-33, 2007
82. Poirier-Quinot M, Frasca G, Wilhelm C, Luciani N, Ginefri JC, Darrasse L, Letourneur D, Le Visage C, Gazeau F, High-resolution 1.5-Tesla magnetic resonance imaging for tissue-engineered constructs: a noninvasive tool to assess three-dimensional scaffold architecture and cell seeding. Tissue Engineering Part C Methods, 16, pp.185-200, 2010
83. Le Visage C, Letourneur D, Method for preparing porous scaffold for tissue engineering, cell culture and cell delivery, International Patent No. PCT/EP2008/063671, filed on 10/10/2008, and issued on 16/04/2009
84. Richter C, Reinhardt M, Giselbrecht S, Leisen D, Trouillet V, Truckenmüller R, Blau A, Ziegler C, Welle A. Spatially controlled cell adhesion on three-dimensional substrates. Biomed Microdevices. 2010 May 18. [published online ahead of printing]

85. Karakecili AG, Demirtas TT, Satriano C, Gümüsderelioglu M, Marletta G. Evaluation of L929 fibroblast attachment and proliferation on Arg-Gly-Asp-Ser (RGDS)-immobilized chitosan in serum-containing/serum-free cultures, J Biosci Bioeng, 104, pp.69-77, 2007
86. Serrano MC, Pagani R, Vallet-Regí M, Peña J, Rámila A, Izquierdo I, Portolés MT. In vitro biocompatibility assessment of poly(epsilon-caprolactone) films using L929 mouse fibroblasts, Biomaterials, 25, pp.5603-11, 2004
87. Knox P, Crooks S, Rimmer CS, Role of fibronectin in the migration of fibroblasts into plasma clots, The Journal of Cell Biology, 102, pp. 2318-23, 1986
88. Ng YKM, Optimization of spatial alignment and surface chemistry of polysaccharide scaffold, BEng Thesis, National University of Singapore, 2010
89. Staat RH, Gawronski TH, Schachtele CF. Detection and preliminary studies on dextranase-producing microorganisms from human dental plaque. Infect Immun, 8, pp.1009-16, 1973
90. Ber S, Torun Köse G, Hasirci V, Bone tissue engineering on patterned collagen films: an in vitro study, Biomaterials, 26, pp.1977-86, 2005
91. Wei J, Igarashi T, Okumori N, Igarashi T, Maetani T, Liu B, Yoshinari M. Influence of surface wettability on competitive protein adsorption and initial attachment of osteoblasts. Biomedical Materials, 4, pp.045002, 2009
92. Aranaz I, Mengíbar M, Harris R, Paños I, Miralles B, Acosta N, Galed G, Heras A, Functional Characterization of Chitin and Chitosan, Current Chemical Biology, 3, pp.203-230, 2009
93. Drumheller PD, Hubbell JA, Surface Immobilization of Adhesion Ligands for Investigations of Cell-Substrate Interactions, The Biomedical Engineering Handbook: Second Edition, Boca Raton: CRC Press LLC, 2000
94. Schaper CD, Nanofabrication with Water-Dissolvable Polymer Masks of Polyvinyl Alcohol (PVA): MxL, Proceedings of SPIE, 5374, pp.325, 2004
95. Lack S, Dulong V, Picton L, Le Cerf D, Condamine E. High-resolution nuclear magnetic resonance spectroscopy studies of polysaccharides crosslinked by sodium trimetaphosphate: a proposal for the reaction mechanism. Carbohydrate Research, 342, pp.943-53, 2007
96. Schruben DL, Gonzalez P, Dispersity Improvement in Solvent Casting Particle/Polymer Composite, Polymer Engineering and Science, 40, pp.139 – 142, 2004
97. Meenakshi et al., Advances in Porous Biomaterials for Dental and Orthopaedic Applications, Materials, 3, pp.2947-2974, 2010
98. David A, The development and the testing of a polyurethane (Biomer) arterial prosthesis, Bulletin of Material Science, 12, pp.33-40, 1989
99. Shalviri A, Liu Q, Abdekhodaie M, Wu XY, Novel modified starch–xanthan gum hydrogels for controlled drug delivery: Synthesis and characterization, Carbohydrate Polymers, 79,pp.898-907, 2010
100. Yow SZ, Quek CH, Yim EK, Lim CT, Leong KW. Collagen-based fibrous scaffold for spatial organization of encapsulated and seeded human mesenchymal stem cells. Biomaterials, 30, pp.1133-42, 2008
101. Yim EK, Wan AC, Le Visage C, Liao IC, Leong KW. Proliferation and differentiation of human mesenchymal stem cell encapsulated in polyelectrolyte complexation fibrous scaffold. Biomaterials, 27, pp.6111-22, 2006

102. Chandran KB, Gao D, Han G, Baraniewski H, Corson JD, Finite-element analysis of arterial anastomoses with vein, Dacron and PTFE grafts. Medical & Biological Engineering & Computing, 30, pp.413-8, 1992
103. Bader, H. Dependence of wall stress in the human thoracic aorta on age and pressure. Circulation Research, 20, pp.354-361, 1967
104. Black J, Hastings GW, Handbook of biomaterial properties, Springer, 1998
105. Gou J, Minaie B, Wang B, Liang Z, Zhang C, Computational and experimental study of interfacial bonding of single-wallwd nanotube reinforced compoistes. Computational Material Science, 31, pp.225-36, 2004
106. Yang A, Wu R, Enhancement of the Mechanical Properties and Interfacial Interaction of a Novel Chitin-Fiber-Reinforced Poly(e-caprolactone) Composite by Irradiation Treatment, Journal of Applied Polymer Science, 84, pp.486–492, 2002
107. Khani MM, Tafazzoli-Shadpour M, Delavearpour S, Naghizadeh Sh, Avolio A, Dynamic stress analysis of the arterial wall utilizing physiological pressure waveforms. American Journal of Applied Sciences, 5, pp. 1285-90, 2008
108. Zhang RZ, Gashev AA, Zawieja DC, Davis MJ. Length-tension relationships of small arteries, veins, and lymphatics from the rat mesenteric microcirculation. American Journal of Physiology. Heart Circulation Physiology 292, pp.H1943-52, 2007
109. Hovgaard MB, Rechendorff K, Chevallier J, Foss M, Besenbacher F. Fibronectin adsorption on tantalum: the influence of nanoroughness. Journal of Physical Chemistry B., 112, pp.8241-9, 2008
110. Carré A, Lacarrière V, How substrate properties control cell adhesion. A physical-chemical approach. Journal of Adhesion Science and Technology, 24, pp. 815-30, 2010
111. Shamloo A, Ma N, Poo MM, Sohn LL, Heilshorn SC. Endothelial cell polarization and chemotaxis in a microfluidic device, Lab Chip,.8, pp.1292-9, 2008
112. Tessa L, Hall H, Cell Guidance by 3D-Gradients in Hydrogel Matrices:Importance for Biomedical Applications, Materials, 2, pp.1058-1083, 2009
113. Sriram P, Kalogerakis N, Behie LA, Experimental determination of the rate of autolysis of trypsin at 37“C. Biotechnology Techniques, 10, pp.601-6, 2004
114. Cai C, Bakowsky U, Rytting E, Schaper AK, Kissel T. Charged nanoparticles as protein delivery systems: a feasibility study using lysozyme as model protein. Eur J Pharm Biopharm. 69, pp.31-42, 2007
115. Bao JJ, Separation of proteins by capillary electrophoresis using an epoxy based hydrophilic coating, Journal of Liquid Chromatography & Related Technologies, 23, pp.61 – 78, 2000
116. Tai BCU, Wan ACA, Ying JY, Modified polyelectrolyte complex fibrous scaffold as a matrix for 3D cell culture. Biomaterial, 31, pp. 5927-35, 2010
117. Siggins RW, Hornick CA, Chapter 15 - Endothelial cell responses to physiological and pathophysiological environments, Anti-Angiogenic Functional and Medicinal Foods, CRC Press, 2007
118. Dobrin PB, Mechanical properites of arteries. Physiological Reviews, 58, pp. 397-460, 1978
119. Tozzi P, Corno A, Hayoz D, Letters to the editor, American Journal of Physiology Heart Circulation Physiology, 278, p.1407, 2000
120. Ishii Y, Sakamoto S, Kronengold RT, Virmani R, Rivera EA, Goldman SM, Prechtel EJ, Hill JG, Damiano RJ, A novel bioengineered small-caliber vascular graft incorporating heparin and

sirolimus: Excellent 6-month patency. Journal of Thoracic and Cardiovascular Surgery, 135, pp. 1237-46, 2008

121. Mohty M, Blaise D, Faucher C, Vey N, Bouabdallah R, Stoppa AM, Viret F, Gravis G, Olive D, Gaugler B. Inflammatory cytokines and acute graft-versus-host disease after reduced-intensity conditioning allogeneic stem cell transplantation. Blood, 106, pp.4407-11. 2005
122. Richardson JV, Mcdowell HA. Anastomotic aneurysms following arterial grafting: A 10-year experience. Annals of Surgery,184, pp.179-82, 1976
123. Keyt BA, Berleau LT, Nguyen HV, Chen H, Heinsohn H, Vandlen R, and Ferrara N. The carboxyl-terminal domain (111–165) of vascular endothelial growth factor is critical for its mitogenic potency. J Biol Chem, 271, pp.7788–7795, 1996.
124. Dvorak HF, Brown LF, Detmar M, and Dvorak AM. Vascular permeability factor/vascular endothelial growth factor, microvascular hyperpermeability, and angiogenesis. Am J Pathol 146, pp.1029–1039, 1995.
125. Clark RAF, Folkvord JM, Nielsen LD, Either exogenous or endogenous fibronectin can promote adherence of human endothelial cells, Journal of Cell Science, 82, pp.263-280, 1986
126. Goerges AL and Nugent MA, pH regulates vascular endothelial growth factor binding to fibronectin: a mechanism for control of extracellular matrix storage and release. The Journal of Biological Chemistry, pp. 2307-15, 2004
127. Staat RH, Gawronski TH, Schachtele CF. Detection and preliminary studies on dextranase-producing microorganisms from human dental plaque. Infect Immun, 8, pp.1009-16, 1973